EXPERIMENTAL MEASUREMENTS AND NUMERICAL PREDICTION OF THE EFFECT OF WAVES ON MOORING LINE FORCES FOR A CONTAINER SHIP MOORED TO PILE SUPPORTED AND SOLID WALL DOCKS

A Thesis

by

ANDRES BAWI SIIN LUAI

Submitted to the Office of Graduate Studies of
Texas A&M University
in partial fulfillment of the requirements for the degree of

MASTER OF SCIENCE

Approved by:

Chair of Committee,	Robert Randall
Committee Members,	James Kaihatu
	Gerald Morrison
Head of Department,	John Niedzwecki

May 2013

Major Subject: Ocean Engineering

ABSTRACT

The conditions of a moored container ship are examined by a physical model in a wave basin and by a numerical simulation. Each condition, wave period, significant wave height and wave direction, was isolated and tested for a 50:1 scale model of a 710 ft ship and model dock. The dock construction, solid sheet wall or pile supported, was varied to add another aspect of a moored vessel. Mooring lines were modeled using 14 springs in typical mooring line arrangement to simulate the elastic properties. Loads experienced on mooring lines and fenders during different wave conditions were recorded using in line force transducers.

Each wave property increased the loads on the mooring lines and fenders as it intensified, except in few conditions. The loads throughout the ship also decreased for the tests run with a pile constructed dock. The bow line received the greatest load and the greatest range of loads of all the lines. The greatest average load was 175 kips experienced by the bow line during a 20 second period, 6 feet wave coming perpendicular to the ship. The results of the solid wall dock setup were compared to the results from the numerical simulation data, aNySIM. Numerical results showed similar trends as the experimental but at a lower magnitude, with a maximum percent difference of 36%.

ACKNOWLEDGEMENTS

I would like to thank my committee chair, Dr. Randall, for his guidance, patience, and mentorship during my time in College Station. Thanks also to my committee members, Dr. Kaihatu and Dr. Morrison, for their support throughout the course of my research.

This research opportunity was made available by PND Engineers. Nels Sultan and Ajay Sampath were on site representatives for PND Engineers, providing consulting and supervision. Paul Johnson, from USM Inc. in Houston, Texas supervised the construction of the container ship model. Arjan Voogt and Wei Xu from Marin USA in Houston, Texas provided training and support for the aNySIM program used for the numerical model. Mr. John Reed provided supervision in the laboratory and assistance with all test instruments, setups, calibrations, and data acquisitions. Four student workers, Shelby Clark, Cory Taylor, Jacob Triska, and Ginny Whisenhunt, assisted with the experiment set up, calibration, and data recording.

TABLE OF CONTENTS

Page

LIST OF FIGURES

Page

LIST OF TABLES

Page

1. INTRODUCTION

Moored container ships are subject to the weather and sea conditions present at their location. Depending on the geographic location of the mooring or the break waters available for protection, these moored vessels are under the mercy of any adverse conditions. This situation can be especially dangerous considering the heavy cargo being transported on and off the ship, and the various stability changes the vessel goes through during a mooring evolution. To better understand the effects that these conditions have on a moored vessel, a model can be run to isolate specific aspects and determine which is the condition that most affects the ship.

The objective of this thesis is to experimentally measure the effects of certain wave characteristics on mooring line and fender loads on a container ship moored to both a solid wall dock and pile supported dock. The wave characteristics tested are significant wave height, significant wave period, and wave direction. The results will then be compared a numerical simulation program called aNySIM in prototype scale.

To simulate the mooring lines and fenders of a vessel, both physical model test and a numerical simulation were used. The physical model test was performed in a wave basin, and a numerical simulation was performed using a program called aNySIM. The loads experienced from various types of wave conditions on the mooring lines and fenders were recorded. The wave conditions isolated certain aspects such as significant wave height, wave period and wave direction. The dock construction was also tested to determine the effect it has on the mooring line and fender loads. Each aspect of the

conditions acting on a moored container ship must be isolated to determine how it affects the ship, and possibly determine the significant conditions to be aware of in future mooring situations.

2. LITERATURE REVIEW

Szelangiewicz (1996) observed the mooring line loads of a vessel, specifically, the dynamic characteristics of these lines. He states that the dynamic characteristics can be approximated by the static characteristics. The static characteristics are a function of the elasticity of the material, pretension, and the weight of 3.2 ft in the air. However, this can only be done when the vessel is experiencing low frequency motions. His observations mainly dealt with steel mooring lines with a high elastic modulus. His experiments did not involve a vessel moored to a fixed structure, rather moored to anchors on the sea bottom. This adds another factor to determining the characteristics of the mooring lines when submerged.

Mansard and Pratte (1982) simulated the nonlinear characteristics of mooring lines using a series of springs and changed their contact points so that as the spring is pulled down, the length of the spring causes a stiffening effect. When scaling the non-elastic characteristics of mooring lines, this method is necessary since it is difficult to model the material of the mooring line. They modeled a 227,000 DWT ship in a 1:100 scale model that was moored using six mooring lines. The mooring lines were modeled using a mix of both springs and nylon rope. The ropes were non-stretching, and the springs were stainless steel. Forces were monitored using force transducers. Essentially, the springs in the (Mansard & Pratte, 1982) experiment were adjusted to give the force on the line as a function of the elongation. The highest RMS force on this

experiment was 51 kips from the forward breast line, with a significant wave height of 8.4 feet.

Pena, et. al. (2011) modeled the forces on the elastic mooring lines of a 65 ft x 13 ft x 6 ft floating breakwater. The test was performed in an 111 ft x 104 ft x 3.6 ft wave tank with three piston type wave generators. They studied forces on the elastic mooring lines with an elastic coefficient of 2,055 lb/ft and 13 ft length. A three dimensional strain gauge was used to obtain the horizontal and vertical shear stresses. Different wave heights, wave periods and wave directions were used for the wave profile to determine the forces on the lines using regular waves. The wave periods tested ranged from 4.8 to 18 s, and tested wave heights ranged from 2.3 to 4.6 ft. The two wave directions analyzed were from 35° and 0°. Also, the pretension on these lines was tested between 10% and 30% of their elongation. The mooring loads in this experiment reached peak values of 14 tons for a 30% pretension line with 35° incident wave angle. It was found that setting a higher pretension only slightly affected the mooring loads (Pena, et al., 2011).

Van der Molen, et. al. (2010) performed a numerical and physical model to study the moored ship motions and forces on mooring lines. The study mainly shows the technologies and methods of the experiment. The experiment scale was 1:100. Along with different wave types, the effect of loaded ships passing the moored vessel was analyzed numerically and physically. The fender forces were measured using Teflon pads, with the correct coefficient of friction, attached to a metal strip that was calibrated to measure forces. The lines were measured using stiff synthetic ropes and springs with

known stiffness factors. The mooring lines were then attached to pulleys on the pier and then to mounted strain (van der Molen, et. al., 2010).Three model were used to simulate a 150,000 Dead Weight Ton (DWT), 205,000 DWT and 320,000 DWT vessels. The ships were ballasted to model the correct center of gravity vertically and horizontally. The moment of inertia was also tested by placing the ship in a cradle. The longitudinal moment of inertia was found by using the observed period during free oscillation. The transverse moment of inertia was found by the free roll period while in the water.

Fernandes, et al. (1998) observed the non-linear properties of polyester mooring cables. Since the cross-sectional area of these cables change in their application on a Floating Production System (FPS), they argued that instead of using the equation for axial stiffness of a line

$$\mathbf{k} = \frac{\mathbf{EA}}{\mathbf{l_o}} \qquad 1$$

it is better to model using the equation

$$\mathrm{k} = \frac{\mathrm{E}}{\rho}\frac{\mathrm{A}\rho}{\mathrm{l_o}} = \frac{\mathrm{E}}{\rho}\frac{\mathrm{d}}{\mathrm{l_o}} \qquad 2$$

where k is the axial stiffness of the line, E is Young's Modulus, A is the cross section area, l_o is the initial line length, ρ is the polymer specific gravity, and d is the mass per unit length of the line. Specifically, the term

$$\frac{E}{\rho}, \qquad 3$$

which is called the Specific Modulus of Elasticity with the units N/tex, following the textile industry unit where 1 tex=10^{-6} kg/m, is the main characteristic of these mooring lines. A rope for a monobuoy that is to be installed in 2,700 ft of water with a minimum

breaking load of about 1,100 kips was tested using multiple methods of loading. The experiments found that the Specific Modulus of Elasticity was a function of the average load, load amplitude and period. These tests all involved submerged mooring lines for the purpose of mooring systems on FPSs.

Randall et. al. (2012)showed the results of an experiment measuring the loads on mooring line forces, fender forces, and motions of a scaled model container ship. The experiment was performed on both a solid wall and pile supported dock. The results indicated there were no significant differences in the forces or motions of a moored container ship on a solid dock compared to a pile supported dock.

3. METHODS*

3.1 Introduction

The physical modeling was conducted in the Haynes Coastal Engineering Laboratory at Texas A&M University in College Station, Texas. A 1:50 model scale was selected as the geometric scale for the vessel and Froude scaling was used for describing waves including significant height, period, and duration. All data were recorded using Lab View data acquisition system. The measured motion and force data at different period height, and direction were compared to results from the aNySIM numerical simulation (Marin, 2012).

3.2 Test Facility

The Haynes Coastal Engineering Laboratory contains a wave tank that is 120 ft long x 75 ft wide x 4 ft deep and a wave generator that can generate regular and irregular waves in up to 1 m water depth using JONSWAP, PM , or TMA spectral shapes. The wave maker's capabilities can be seen in Table 1. A picture of the wave basin from the Southeast corner is shown in Figure 1.

* Reprinted with permission from "Comparison of Laboratory and Predicted Motions and Mooring Line Forces for a Container Ship Moored to Dock" by Y. Zhi and A. Luai, 2013, 2013 SNAME Texas Section Offshore Symposium.

Figure 1. Wave Basin in the Haynes Coastal Laboratory from the Southeast corner

Table 1. Haynes Laboratory Directional Wave Generator Capabilities

Regular	**Spectral**
Period range of 0.5 to 5 s	Sig wave height 0.98 ft at peak period 3.0 s
Wave height 1.31 ft at 1.5 s	Sig wave height 1.18 at peak period 2.3 s
Wave height 1.64 ft at 3 s	
Angle of propagation 0 to 60 deg	
Wave height 1.94 ft at 2.4 s	
Wave height 1.31 ft at 5 s	

A general layout of the wave basin is illustrated in Figure 2. On the west end of the facility, there is a directional wave generator that contains 48 paddles. The waves propagate to the test site and then are absorbed at the east end by the rock beach.

The data acquisition instrument carriage is where the data from the mooring lines and fenders are received and monitored. The force transducers are physically wired from transducer locations on the model vessel up to the Lab View data acquisition

system on the carriage. The carriage also monitors the wave heights in the basin using capacitance wave gauges, and the wave data is recorded with the same data acquisition.

Currents can also be generated in this laboratory. Immediately east of the wave generator, there are removable floor panels. Depending on the amount of current desired, the floor panels can be removed, allowing for water to flow out from the opening resulting from panel removed. Water is simultaneously discharged over weirs to the collection tank at the East end of the wave basin, where the rock beach is located. The water is returned to the suction side of the four axial flow pumps via a 4 ft diameter pipe connected to the collection tank. The pump speed is controlled to achieve the desired current velocity. The four axial flow pumps can pump up to 35,000 GPM.

3.3 Model Ship

The geometric scale of this experiment is 50:1. Since the model is geometrically undistorted, all lengths are scaled down by 50. To scale the prototype wave periods to model size, Froude scaling was used. The Froude number (Fr) is

$$\mathrm{Fr} = \frac{\mathrm{V}}{\sqrt{\mathrm{gL}}} \qquad 4$$

where V is the velocity, g is the acceleration due to gravity, and L is the length. Using the Froude scaling method, the time scale can be found with the known geometric scale of 50:1 since

$$\mathbf{Fr_m} = \mathbf{Fr_p} \qquad 5$$

$$\frac{V_m}{\sqrt{g_m L_m}} = \frac{V_p}{\sqrt{g_p L_p}} \qquad 6$$

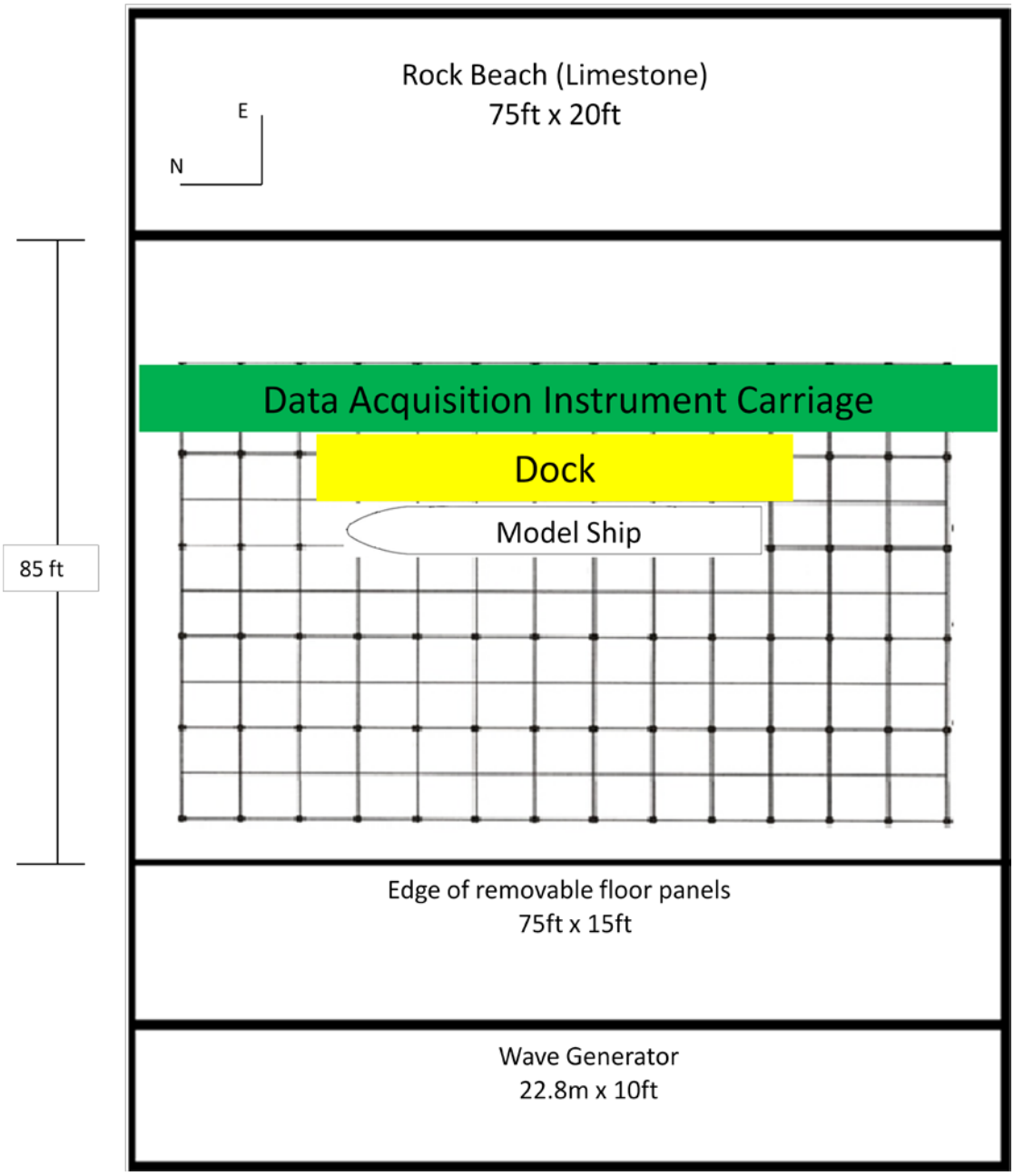

Figure 2: Wave Basin with Approximate Location of Instrument Carriage, Model Dock, and Model Ship

where m and p denotes model and prototype. Since acceleration due to gravity is the same in both model and prototype,

$$\frac{V_m}{\sqrt{L_m}} = \frac{V_p}{\sqrt{L_p}} \quad (7)$$

$$\left(\frac{V_p}{V_m}\right)^2 = \frac{L_p}{L_m} \quad (8)$$

$$(N_v)^2 = N_l \quad (9)$$

Since the geometric ratio is equal to the square of the velocity ratio, and the time ratio is equal to the length ratio divided by the velocity ratio,

$$N_t = \frac{N_l}{N_v} \quad (10)$$

Then,

$$N_t = \frac{N_l}{\sqrt{N_l}} = \frac{N_l}{{N_l}^{1/2}} \quad (11)$$

$$N_t = \sqrt{N_l} \quad (12)$$

Since the length scale ratio is 50, the time scale is √50, or 7.07. To scale the hydrodynamic forces of the model ship, the specific weight ratio of salt water and fresh water was assumed to be equal. The specific gravity ratio is equal to 1, $N\gamma=1$. Using the hydrodynamic forces equation (Hughes, 1993), the hydrodynamic forces can be modeled.

$$N_F = N_\gamma (N_l)^3 \quad (13)$$

$$N_F = (N_l)^3 \quad (14)$$

The hydrodynamic force ratio is equal to the geometric scale ratio to the third power. So, the weight of the model ship is 50^3, or 125,000, times less than the prototype weight. The specifications of the model and the prototype ship for both Froude scale and geometric scale are tabulated in Table 2.

Table 2. Model ship and Dock and Wave Basin Conditions for Selected Geometric Scale and Froude Scale

Ship Characteristics	**Prototype**	**Prototype Units**	**Model Ship**	**Model Units**
Displacement	37474	tons	599.58	lbs
Length	710	ft	170.4	inches
Beam	78.21	ft	18.77	inches
Depth	51	ft	12.24	inches
Draft (typical), (light)	28, 13	ft	6.72, 3.12	inches
Environment Conditions				
Water depth	50	ft	12	inches
Water depth +high tide	58.8	ft	14.4	inches
Quayside distance	8	ft	1.92	inches
Significant wave heights	2,4,6,8,10	ft	0.48, 0.96, 1.44, 1.92, 2.40	inches
Wave periods	4,6,8,10,12, 14, 16, 18, 20	s	0.57,0.85, 1.13, 1.41, 1.70,1.98, 2.26,2.56	s

The prototype container ship modeled is weighs approximately 18.5 tons. Two different drafts were tested; however, the results are not reported here. The conditions tested range from significant wave heights of 2 ft to 10 ft in increments of 2 ft and wave

periods from 4 to 20 seconds in prototype scale. The model ship was custom made with a bulbous bow, rudder, and seven compartments accessible from the top deck as shown in Figure 3. The seven compartment openings are ballast holes used to place weights in order to ballast the ship to achieve a particular draft. There are also draft markings on the hull at the bow, amidships, and stern. The change in color between maroon and yellow on the hull is at the 6.75 inch draft line.

Figure 3. Model Ship in Empty Wave Basin

The model ship was ballasted to a draft line of 6.75 inches that represents the fully loaded draft, which equates to a prototype draft of 28 feet. Lead weights were distributed throughout the seven compartments through each ballast hole (H1-H7) to obtain this draft evenly, without a list or permanent pitch. The light ship vertical center of gravity (CG) for the model ship is marked in Figure 4 as point 1. Point 2 is the

vertical CG after ballasting the ship to the draft of the fully loaded ship. Point 3 shows the vertical CG for the 13 feet draft load test. Table 3 shows the weight distribution in every compartment. Table 4 shows the calculations to compute the center of gravities. VCG, VCB, LCG, LCB, TCG, TCB, GM, and T represents the vertical center of gravity, vertical center of buoyancy, longitudinal center of gravity, longitudinal center of buoyancy, transverse center of gravity, transverse center of buoyancy, metacentric height, and period, respectively. The center of gravity, for both vertical and longitudinal, were calculated by taking the new moment created by the known weight and distance of the lead weight and where it was placed, and dividing it by the sum of the weights. All vertical measurements are from the keel; the longitudinal measurements are measured from the bow; and the transverse measurements are measured from the centerline.

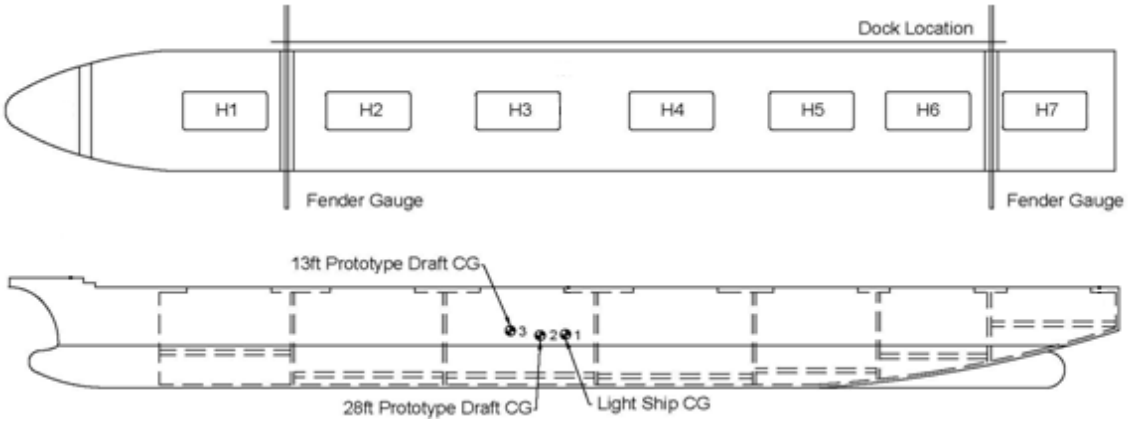

Figure 4. Model Ship Showing Ballast Holes, Center of Gravity, and Shelves for Ballast Weights

Table 3. Weight Distribution

Location	Prototype 28 ft draft (Model 6.75 inch draft) (lb)	Prototype 13 ft draft (Model 3.25 inch draft) (lb)
Light Ship	176.0	176.0
Fender gauge forward	1.2	1.2
H1	66.8	15.5
H2	33.1	13.2
H3	60.0	6.9
H4	115.3	4.6
H5	60.0	3.7
H6	9.1	0
H7	0	0
Fender gauge aft	1.2	1.2
Total Displacement	522.7	222.3

Table 4. Model Ship Characteristics for Two Different Drafts

Characteristic	Model Ship		Model Scaled up to Full Size Ship	
	(Model 6.75 inch draft)	(Model 3.25 inch draft)	Prototype 28 ft draft	Prototype 13 ft draft
VCG (ft)	0.465	0.636	23	32
VCB (ft)	0.34	0.34	17	17
LCG (ft)	6.74	6.518	337	337
LCB (ft)	6.76	6.52	338	338
TCG (ft)	0	0	0	0
TCB (ft)	0	0	0	0
GM (ft)	0.15	0.19	7.5	10
T_r (s)	1.8	2	13	14

3.4 Model Docks

The solid dock was modeled by using concrete masonry blocks (CMU). The blocks were stacked two high with a wood surface on top. The curves on the sides of the dock were made from PVC sections that were cut 1.4 feet high and 8 inches wide. There

are seven fenders spread evenly on the dock to prevent excessive load on the dock and prevent damage to the ship. These fenders act like the tire fenders on docks. The center fender is where the centerline of the ship is located. The gravel on both ends of the dock is sloped to simulate the prototype dock. There is also gravel on the toe of the dock to simulate scour protection. The plan and elevation view of the model ship and pier can be viewed in Figure 5 and Figure 6.

The ship was also moored to a pile constructed dock. The dock consists of 36 PVC tubes that support the platform of the dock, which simulates the wood piles actually used to construct the dock. Concrete masonry unit blocks are placed behind the dock. Gravel is sloped down from these blocks to form model the armor rock. Gravel was also placed on the toes of the piles to form the scour protection. The plan and elevation view of the model ship and pill pier can be viewed in Figure 7 and Figure 8.

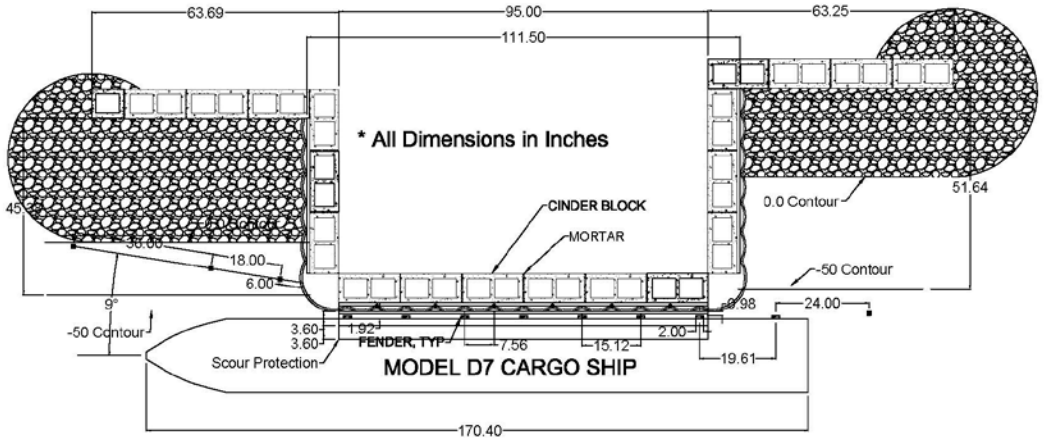

Figure 5. Plan View of the Model Solid Wall Dock

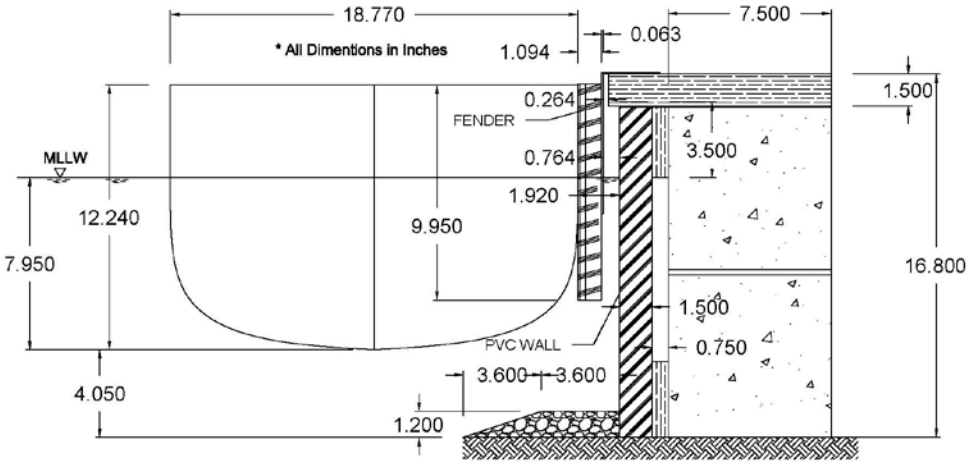

Figure 6. Elevation View of Model Solid Wall Dock

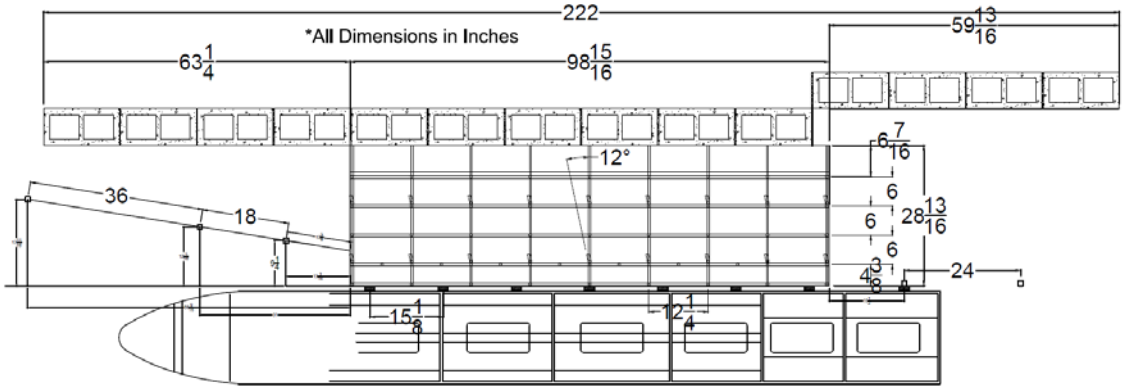

Figure 7. Plan View of Model Pile Wall Dock

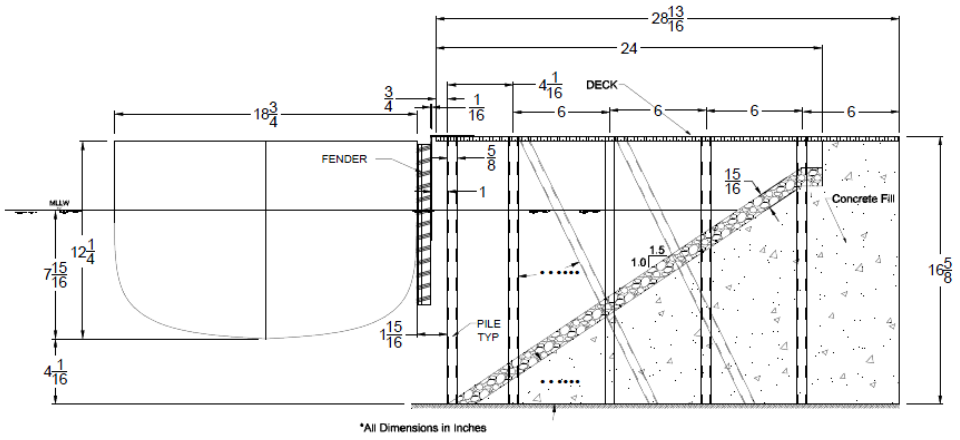

Figure 8. Elevation View of Model Pile Wall Dock

3.5 Mooring of Model Container Ship to the Dock

The model ship was moored to the solid wall dock using wires and springs to simulate the prototype mooring system that consisted of synthetic mooring lines. A schematic of the model's fourteen synthetic line mooring system is illustrated in Figure 9. There were three bow lines (1a, 1b, and 1c) and two forward breast lines (2a and 2b). Two spring lines were forward (3a and 3b) and two spring lines were aft (4a and 4b). Lines 5a and 5b were the aft breast lines, and lines 6a, 6b, and 6c were the stern lines. The model mooring lines consisted of 0.072 inch outside diameter wire rope, a 0.75 inch outside diameter coiled spring with appropriate spring constant, and wire rope from the spring to the connector on the mooring dolphin. The mooring dolphins were 0.75 inch diameter galvanized steel rods welded to a 1.5 ft square plate. The plate was weighted with rock and lead weights. Each dock had seven fenders spaced similarly to the prototype dock. The fenders were constructed with wood, cushioning material, and a

thin Plexiglas cover. The fenders were attached to the dock using 90 degree steel angles. One additional fender was attached to first aft mooring dolphin and rested against the stern of the model ship.

Mooring line forces were measured in four of the mooring lines (1a, 3a, 4a, and 6b) using tension load cells. The load cells in the spring lines (3a and 4a) were 5 lb capacity and for the bow line (1a) and stern line (6b) were 10 lb capacity. Two fender gauges were used and attached to the model ship forward and aft as shown in Figure 10. The fender gauge rested on an 8 inch by 10 inch plate constructed similar to the fenders. The fender gauge consisted of a spring and load cell and a roller ball that rested on the two fender plates. The capacity of the fender gauges was 40 lb. The model spring constants are tabulated in Table 5.

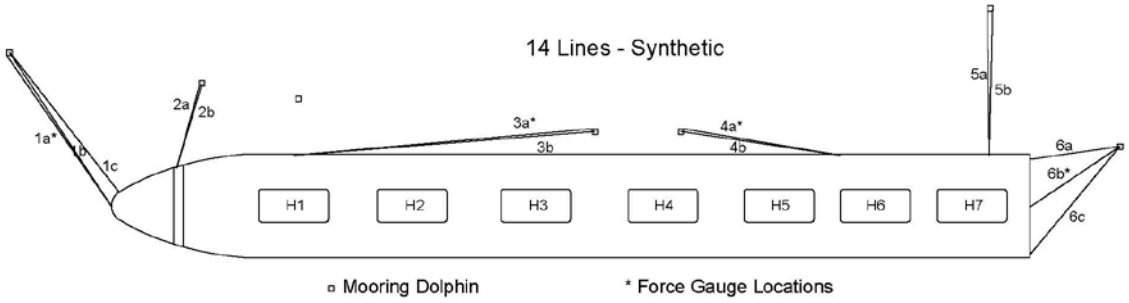

Figure 9. Schematic of Mooring Line Locations

Table 5. Model Mooring Line Spring Constants

Line	Spring Constant (lb/in)	Line	Spring Constant (lb/in)
1a	1.37	4a	2.73
1b	1.37	4b	2.73

Table 5. (cont.)

Line	Spring Constant (lb/in)	Line	Spring Constant (lb/in)
1c	1.37	5a	8.19
2a	1.64	5b	8.19
2b	1.64	6a	2.05
3a	2.73	6b	1.64
3b	2.73	6c	1.37

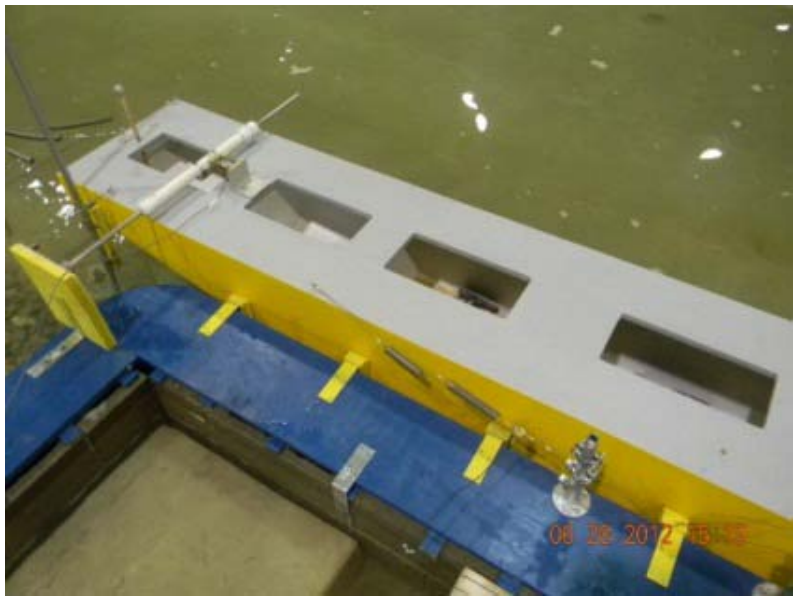

Figure 10. After Fender and Fender Gauge in Solid Dock Configuration

The fourteen mooring lines for the prototype container ship were distributed as follows: 3 bow lines, 2 forward breast lines, 2 forward spring lines, 2 aft spring lines, 2 aft breast lines, and 3 stern lines. The lines are from a Samson, Ultra Blue, 2-5/8 inches diameter, 8 strand ropes. This line has a breaking strength of 140,000 pounds (Samson Rope, 2011). The determination of the spring constant required modeling the mooring lines and evaluating the elasticity of the mooring line. Since this rope has a breaking

strength of 140,000 pounds and cross sectional area is 5.41 square inches, a stress strain curve was created. Using this method, the slope of this line, which is the elasticity, is found to be 194,406 psi. Using the approximate modulus of elasticity for an 8x19 wire rope (8 strands with 19 wires each) with a fiber core from the Hanes Supply Inc. (2002), the elasticity of the wire ropes (line 3, 4a, 5b, and 6) were determined to be 8.10×10^6 psi.

All 14 springs were placed in their respective locations, making sure that doubled-up lines do not have their springs touching. Another precaution was to make sure the force transducers, which were installed on line 1a, 3a, 4a, and 6b had clearance for unobstructed movement during the test. Lines 1a and 6b had a 10 lb capacity force gauge inserted in-line between the spring and wire, and lines 3a and 4a had a 5 lb force transducer capacity inserted. The force transducers output a voltage to the data acquisition system. The force transducers were calibrated to convert from voltage to pounds.

All of the lines have a pretension load of 0.5 pounds. With the known spring constant, the exact elongation for the spring can be calculated to achieve 0.5 pounds of pretention, model scale. Each mooring line was then elongated a length specific to each line before beginning the experiments.

Now that the elasticity of the prototype mooring line is known, the elasticity of the model mooring line can be calculated. The elasticity of the model was determined using the equation

$$E_m = \frac{E_p(N_L)^2}{N_{F_H}} \qquad 15$$

E_m is the model's elasticity, E_p is the prototype's elasticity, N_L is the length scale ratio, and N_{FH} is the hydrodynamic force scale (Hughes, 1993). The length scale ratio is given as 50. The hydrodynamic force scale ratio was determined using

$$N_{F_H} = \frac{SG_{sw}}{SG_{FW}}(N_L)^3 \qquad 16$$

where SG_{SW} and SG_{FW} are the specific gravity of salt water and fresh water, respectively. In order to find the required spring constant that would accurately simulate this elasticity, the original length of the spring line must be determined. The length of each line is according to the mooring plan shown in the previous Figure 9. The respective model length and required spring length are shown in Table 6.

Table 6. Comparison of Prototype and Model Mooring Line Characteristics

	Proto Length (ft)	**Model Length (in)**	**Spring Length (in)**	**k (lb/in)**
Line 1a	160	36	6	1.37
Line 1b	160	36	6	1.37
Line 1c	160	36	6	1.37
Line 2a	65	17	5	1.64
Line 2b	65	17	5	1.64
Line 3a	185	61	3	2.73
Line 3b	185	61	3	2.73
Line 4a	185	29	3	2.73
Line 4b	185	29	3	2.73
Line 5a	10	5.5	1	8.2
Line 5b	10	5.5	1	8.2
Line 6a	65	15.7	4	2.05
Line 6b	85	18.9	5	1.64
Line 6c	110	25.5	6	1.37

With the required spring length that spans from the ship to the dock, the model spring constant was calculated using the equation

$$k = \frac{E_m A}{L} \quad (17)$$

where A is the initial cross sectional area and L is the unstretched length of the spring. A set of cut-to-length springs were ordered with a 0.75 in outer diameter, 0.072 in wire diameter with a rate constant of 8.7. Using a Poisson ratio for the material of 0.29, the known modulus of elasticity of $3x10^7$psi, the shear modulus, G, was found to be $1.16x10^7$ psi. The number of coils in each spring in each line was calculated by solving for N in the equation

$$G = \frac{kNR^3}{r^4} \quad (18)$$

where k is the spring constant, R is the radius of the spring, and r is the radius of the wire. The spring is cut accordingly. In order to get a more accurate spring constant, the springs were tested by measuring the distance traveled for increasing increments of weight.

With the correct size spring to represent every mooring line, the springs were installed between the model dock and mooring dolphins and the model container ship. The positioning of the mooring lines on the ship was determined using an example container ship. This example ship had the same mooring line layout; however, this ship was slightly greater in length. In order to accurately portray the prototype, the relative location of the mooring lines was estimated for the model ship. For example, if the aft breast line was located about 2/3 of the way down from the bow of the example ship, then the aft breast line was also located 2/3 of the length of the model ship. The actual

location of the mooring lines on the ship and its fixed point on the pier are shown in the previous Figure 9.

The model ship and dock structure were placed near the center of the tank parallel to the wave generator, and the instrument carriage was positioned behind the model for best viewing by the four motion tracking cameras. Weights were placed inside the model ship to obtain proper weight and center of gravity with respect to X, Y and Z axes. The model ship was moored to the dock using wires and springs to simulate the prototype mooring systems. Four Futek force gauges and two fender gauges were used to measure the forces in four mooring lines and two fenders. Two video cameras were used to video record the movement of the model ship moored to the dock during waves. One camera viewed the bow of the model ship and the other viewed the beam.

The force gauges were calibrated at the start of each test day. The wave files were generated before testing and loaded into the wave generation computer prior to each test. The water depth was adjusted each morning using the average of the 48 water level gauges on the front of each wave paddle. The tests were for a time length of 8 minutes except for four tests that were for 24 minutes, or 56 mins and 2 hrs 50 mins in prototype scale. A period of 3-5 minutes before the next test was allowed for the water in the wave basin to return to the calm still water condition before the next test was initiated.

3.6 Instruments

The water level in the basin is set before the tests begin using 36 inch capacitance wave gauges. The calibration tool is an system that automatically takes five data points

using a known water depth. The loads on the mooring lines are measured using Futek load cells. Depending on where the load cell is placed, the cell is rated at 5 lbs, 10 lbs and 40 lbs. All of these data signals are received by the 16 channel Lab View data acquisition system that is stationed on the data acquisition carriage.

3.7 Calibration Procedures

The capacitance wave gauges were calibrated by an automatically controlled system which takes five measurements based on the given water depth. With the five data points, a point-intercept line can be formed. The resulting slope is used as the calibration curve used to translate readings from the wave gauge to an actual depth. Once the calibration is complete, three wave gauges were placed in a line perpendicular to the model ship and at a distance of three wave lengths away from the wave generator, as recommended in (Mansard & Funke, 1980). The calibration device and wave gauge setup is depicted in Figure 11.

Figure 11. Wave Calibration Machine (left) and Wave Gauge Setup (right)

There were three different types of load cells used in this experiment. Two load cells were rated at 5 lb capacity, two load cells were rated 10 lb capacity, and two load

cells were rated at 40 lb capacity. All the load cells were calibrated the same way. The load cells were connected to the LabView data acquisition program while multiple known loads were added in increasing order, using a weight hanger. The voltage reading from the data acquisition program is recorded with its corresponding weight. Each load cell was calibrated. An example calibration curve can be seen in Figure 12. The results of the calibration are shown in Table 7.

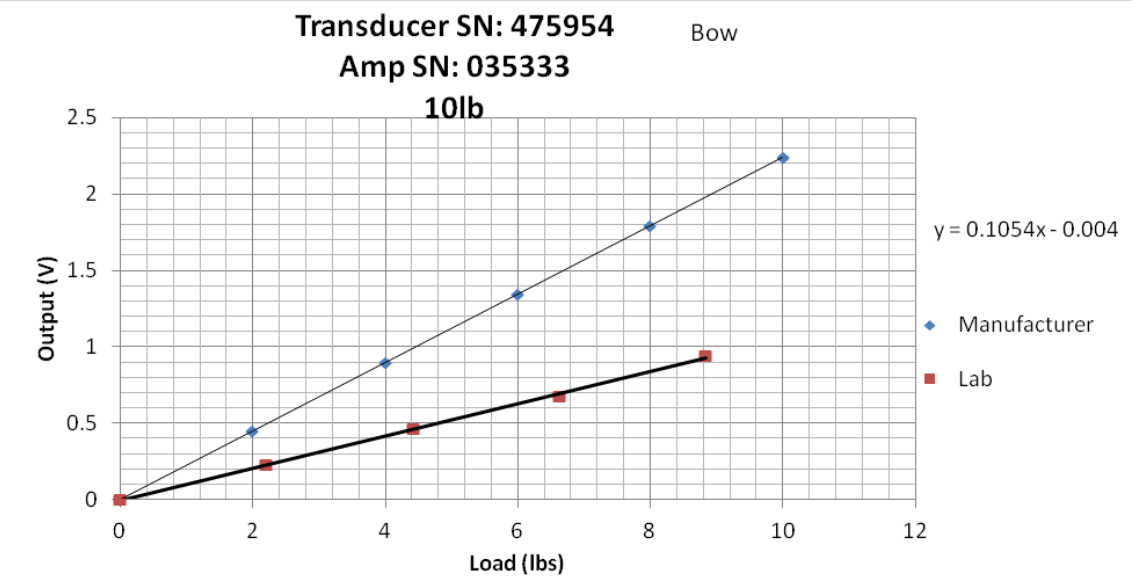

Figure 12. Calibration Curve of Load Cell on Bow Line

Table 7. Load Cell Calibration Data

Bow		FWD Spring		AFT Spring		Stern		FWD Fender		AFT Fender	
Load (lbs)	Lab output (V)	Load (lbs)	Lab output (V)	Load (lbs)	Lab output (V)	Load (lbs)	Lab output (V)	Load (lbs)	Lab output (V)	Load (lbs)	Lab output (V)
0	0	0	0	0	0	0	0	0	0	0	0
2.21	0.23	2.21	0.37	2.21	0.37	2.21	0.22	2.21	0.19	2.21	0.19
4.42	0.46	4.42	0.75	4.42	0.75	4.42	0.45	4.42	0.37	4.42	0.38
6.63	0.68					6.63	0.67	6.63	0.56	6.63	0.58
8.84	0.94					8.84	0.94	8.84	0.75	8.84	0.77
								11.1	0.94	11.1	0.96

The two spring lines have only three data points because the load it was rated for was only 5 lbs. The bow, stern and both fender load cells had at least 5 data points to create a best fit linear curve. The load cells were then placed in line with the springs. Before beginning testing, the load cells were zeroed each day on the signal conditioning unit. The load cells in line with the springs and the fender can be seen in Figure 13.

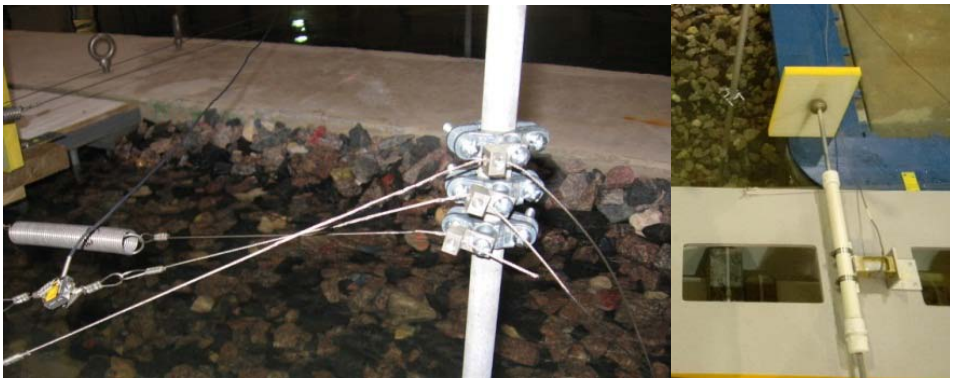

(a) (b)

Figure 13. Close Up of Mooring Line Load Cell (a) and Fender Force Gauge (b)

In order to precisely model the elasticity of the mooring lines using springs, the exact number of coils in every spring for all 14 lines were calculated. Equation 17 is modified to solve for k.

$$k = \frac{Gr^4}{NR^3} \qquad 19$$

The number of coils, N, of each spring is counted and used along with the other known variables, wire radius, r, spring radius, R, and modulus of rigidity, G. The computed rate from equation 19 is compared with its respective target spring constant as specified in Table 5. If the computed rate is within 10%, further calibration is performed. A known weight is placed on the spring using a weight holder, and the elongation was recorded, as shown in Figure 14. The weight was increased by increments and the elongation recorded so that 6 data points were found. The slope of the line from the elongation vs weight added is the spring constant. Due to the 10% error initially, the actual spring constant was found to be lower than the target rate. The percent error between the target spring constant and the actual spring constant is used to find the exact number of coils that needs to be removed. Once removed, the process is repeated until a percent error of below 3% is obtained (Felderhoff, 2012).

Figure 14. Spring Calibration Setup

3.8 Test Procedures

After the calibration of the wave and force gauges, and after the proper water level was verified, the wave profile for that day's testing was loaded into the wave generation computer. With all gauges and data acquisition programs running, the wave generator started. The tests ran for 8 minutes with the exception of four tests that ran for 24 minutes, which equates to about 50 minutes and 1 hour and 2 hours, respectively, in the prototype scale. After every test, a period of 3 to 5 minutes was used to allow the water in the basin to calm. The next test followed after the water was sufficiently calm.

The experiment involved 54 tests; however, only select variables are discussed in this thesis. The details of all 54 tests can be found in Kodiak Pier 3 - Ship Motion Tests

for a Solid Fill and Pile Supported Pier, 2013. The details of the tests discussed in this paper can be found in Table 8 in prototype values. Each test was performed once for the solid dock configurations and repeated using the solid dock configuration. Tests 3, 21, and 36 are the baseline tests with the same significant wave height, period and direction of 6 ft, 12 s, and 0°, in prototype scale, respectively. Most tests have the mooring line with a pretension of 0.5 lbs, model scale. However, some lines do not have pretension, which are designated as "loose," which indicates no pretension. Forces on the mooring lines were not obtained during the first ten tests during the solid dock configuration.

Table 8: Relevant Test Plans for Solid and Pile Dock Setups in Prototype Scale

Test	Duration (minutes)	Draft (ft)	Hs (m)	T (s)	Dir (deg)	Spectra Peak Factor
3	57	28	6	12	0	3.3
6	57	28	6	4	0	3.3
7	57	28	6	6	0	3.3
8	57	28	6	8	0	3.3
9	57	28	6	10	0	3.3
10	57	28	6	14	0	3.3
11	57	28	6	16	0	3.3
12	57	28	6	18	0	3.3
13	57	28	6	20	0	3.3
14	57	28	2	12	0	3.3
15	57	28	4	12	0	3.3
16	57	28	8	12	0	3.3
17	57	28	6	12	-30	3.3
18	57	28	6	12	-15	3.3
19	57	28	6	12	15	3.3
20	57	28	6	12	30	3.3
21	57	28	6	12	0	3.3
36	57	28	6	12	0	3.3

3.9 Numerical Model (aNySIM)

The numerical model used to find the numerical results, aNySIM, was developed by Marine Research Institute Netherlands, Marin. The numerical model was used to analyze the mooring line forces at the prototype scale using given inputs (Marin, 2012). The inputs include the vessel's characteristics such as dimensions, stability dimensions, displacement, damping and hydrodynamic properties. The mooring lines are then input into the program using the reference coordinate system for the start and end points. The elasticity curve, breaking strength, and pretension data for each line are selected. Fender location, size, and friction characteristics are also chosen.

Using those set specifications of the ship, mooring lines and fenders, multiple wave conditions can be used to run the simulation. Significant wave height, wave period, wave type, and direction can be selected depending on the variable to be tested. Wind and current inputs are also adjustable, depending on the test. A simulation of only the solid wall dock was performed.

4. RESULTS*

4.1 Numerical vs. Experimental

The effects of wave height, wave period and wave direction in the experimental and numerical tests are discussed.

4.1.1 Effect of Wave Height

Tests 14, 15 and 16 used the same wave to test the mooring line forces with the exception of the wave height. The wave period is kept constant at 12 seconds while the wave height for test 14, 15 and 16 in the prototype scale are 2 ft, 4 ft, and 8 ft respectively. The average percent difference between the numerical and experimental results are 19%, 27%, and 15% for lines 1a, 3a, and 6b, respectively. From Figure 15, it is observed from the numerical method that as wave heights increase, the loads on the lines increase. The experimental data also agree with this trend, except at line 6b, where the average load for a 4 ft wave is less than the 2 ft wave. This could be due to an experiment or calibration error from the force transducers. Although the upwards trend in average load for the two methods agree with each other, there is still a high average percent difference because the loads for the experimental method are higher across every test.

---

* Reprinted with permission from "Comparison of Laboratory and Predicted Motions and Mooring Line Forces for a Container Ship Moored to Dock" by Y. Zhi and A. Luai, 2013, 2013 SNAME Texas Section Offshore Symposium.

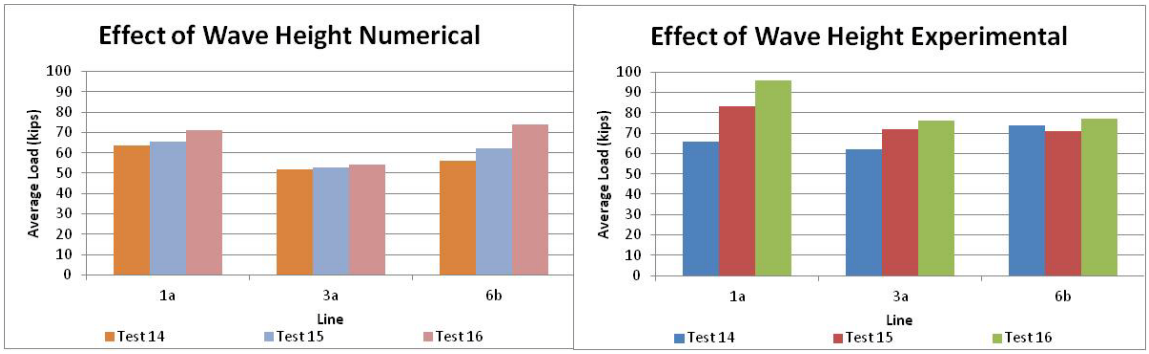

Figure 15. Effect of Significant Wave Height (2 ft, 4 ft, 8 ft, for tests 14, 15 and 16, respectively) with Constant Period (12 sec) on Mooring Lines in prototype scale

4.1.2 Effect of Wave Period

The results of the average load on lines 1a, 3a, and 6b from varying wave period while keeping significant wave height constant is shown in Figure 16. Line 1a has an observable gradual increase in load as the wave period increases for both the numerical and experimental methods. The only exception is for test 13 of the experimental method. There is no clear trend in mooring line loads in the other lines as the wave period increases for either the experimental or numerical tests. The test methods do not agree with each other with an average percent difference of 20%, 30%, and 16% for lines 1a, 3a, and 6b, respectively. The average loads for all tests on lines 3a and 6b for the experimental method are greater than the loads on the corresponding lines and test numbers for the numerical method.

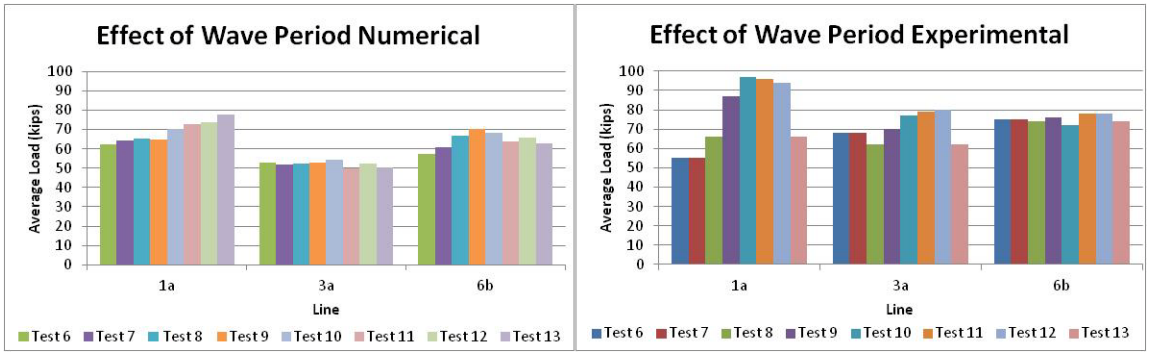

Figure 16. Effect of Wave Period (Ranging from 4 sec to 20 sec in Even Increments from Test 6 to Test 13, Respectively) with a Constant Significant Wave Height (6 ft) on Mooring Line Forces in Prototype Scale

4.1.3 Effect of Wave Direction

On this test, the wave direction came from a range of -30 degrees to 30 degrees, where 0 degrees is the angle of the wave coming perpendicular to the vessel. Test 21 is the control test (wave direction=0 degrees) and tests 17 to 20 have wave directions from -30 degrees to 30 degrees, as shown in Figure 17.

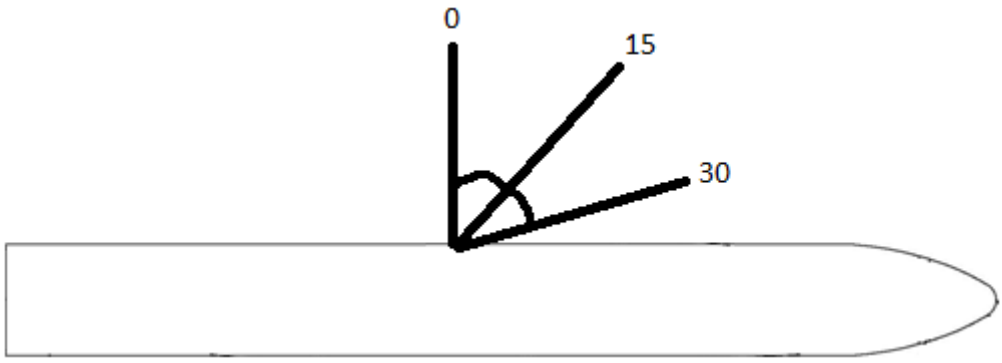

Figure 17. Wave Direction Reference

The results of the tests are illustrated is Figure 18. In the numerical model, the different wave directions did not have an effect on the mooring lines. The standard deviation of the average load in line 1a, 3a, and 6b of every test for the numerical model is 2, 1, and 2 kips, respectively. However, the corresponding values for the experimental method are 14, 4 and 4 kips, respectively. Although the standard deviation of the experimental data shows there are differences between the tests, there is no clear trend or systematic change as the wave direction changes. The numerical data show more consistency between the tests at each line, and that the average load is lower throughout the tests for each line compared to the experimental data. The average percent difference between the tests at lines 1a, 3a and 6b are 21%, 26% and 8%, respectively. Only the average loads on line 6b for the numerical and experimental data show some similarity between the tests than compared to the other lines of either experimental test or numerical simulation.

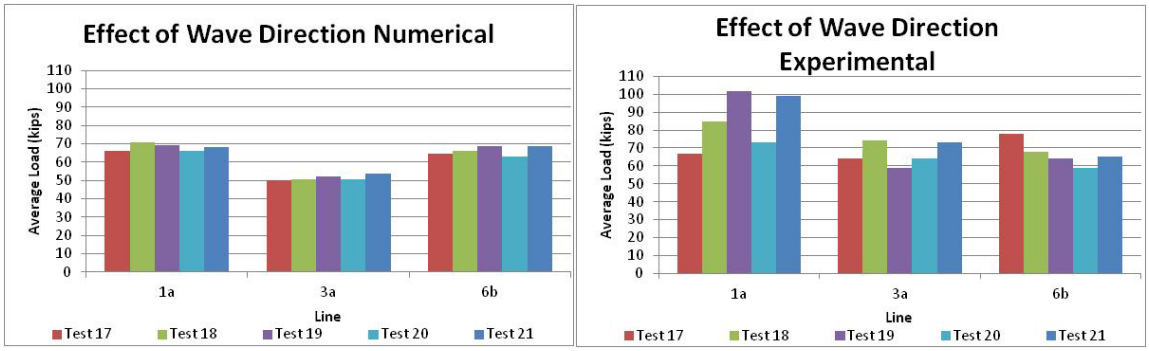

Figure 18. Effect of Wave Direction on Mooring Line Forces

4.2 Pile vs Solid Dock Configuration

The effects of wave height, wave period and wave direction in the pile and solid dock configuration are discussed.

4.2.1 Effect of Significant Wave Height

The loads on the bow, spring and stern lines were less on the pile dock setup than on the solid dock setup. The average percent difference between the forces on the lines on the solid and pile docks for lines 1a, 3a, and 6b were 24%, 14%, and 10%, respectively. Only the stern line, 6b, showed loads similar to the solid dock setup. Although the effects of the significant wave heights on the loads on the pile dock setup were less than that on the solid dock setup, the upwards trend as the significant wave height increases is maintained, as seen on Figure 19.

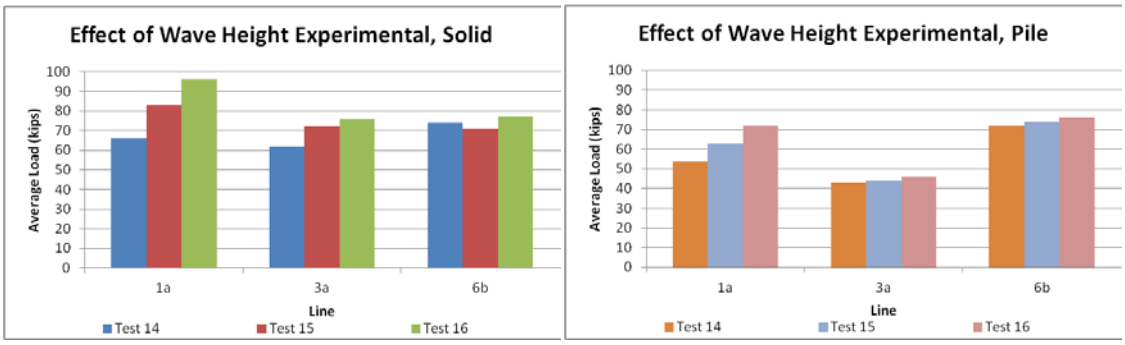

Figure 19. Effect of Significant Wave Height on Mooring Line Forces

4.2.2 Effect of Wave Period

The wave period test on the pile dock setup also showed the same trend as compared to the significant wave height results. The average loads on the mooring lines

in the pile dock setup are lower than the loads on the solid dock setup. The percent difference between loads on the two types of docks for lines 1a, 3a, and 6b are 27%, 48% and 12%, respectively. An upwards trend in loads as the wave period increases is easily determined on the pile dock setup as opposed to the solid wall setup. This trend is evident in the bow and spring lines for both docks. However, tests 12 and 13, which has a wave period of 18 and 20 seconds in the prototype scale, respectively, does not show this trend. The loads on line 6b on both dock setups do not show this upwards trend, as shown in Figure 20.

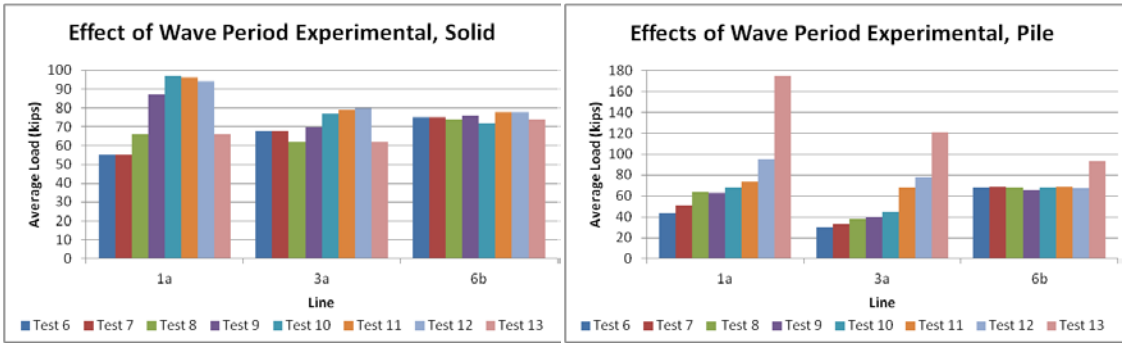

Figure 20. Effect of Wave Period on Mooring Line Forces

4.2.3 Effect of Wave Direction

The loads on the mooring lines on the pile dock setup, as compared to the solid dock setup, show a similar trend for lines 1a and 3a. Both dock setups in line 1a show that the loads are greater at 15° than at 30°. In line 3a, the trend shows that the load increases from +30° to +15° but decreases from -15° to -30°. This trend was observed for both solid dock and pile dock setups. The differences between the loads on the

mooring lines on the pile dock setup, as compared to the solid dock setup, are not as evident in line 6b. The percent error between the loads on lines 1a, 3a, and 6b are 24%, 14%, and 10%, respectively. Loads in lines 3a and 6b are relatively similar between the two dock setups. However, like the loads in the solid dock setup, the loads in the pile dock setup do not show any trend as the wave direction changes, as shown in Figure 21. Test 17, 18, 19, 20 and 21 have wave angles of +30°, +15°, -15°, -30°, and 0°, respectively.

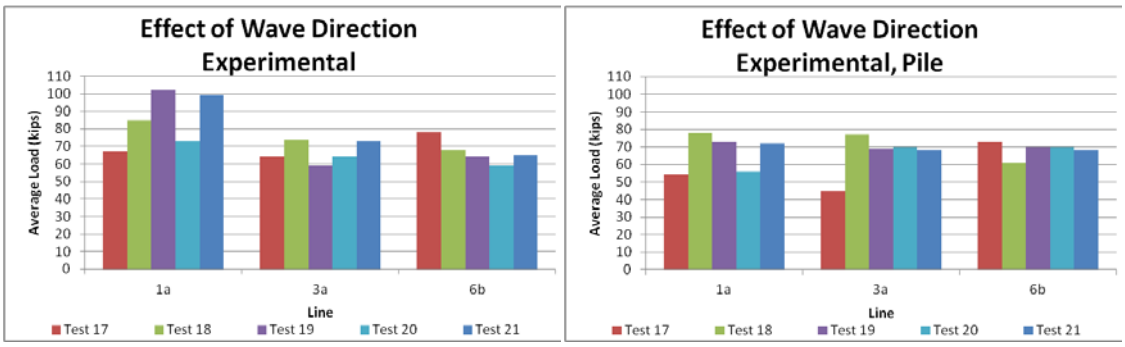

Figure 21. Effect of Wave Direction on Mooring Line Forces

5. DISCUSSION

The mooring lines of a model container ship moored to both a solid dock and pile supported dock were tested using multiple types of waves. Different aspects were kept constant in order to isolate the impact of the significant wave height, wave period, and wave direction have on mooring lines and fenders. Data on the first ten tests during the solid dock configuration were not obtained. The complete results of all mooring line and fender forces of both dock configurations are compared side by side and can be observed on Appendix A.

5.1 Numerical Results Comparison

For mooring line forces, the numerical method shows that as wave heights increase, the loads on the lines increase. The experimental data also agree with this trend. The average loads for all tests on lines 1a, 3a and 6b for the experimental method are greater than the loads on the corresponding lines and test numbers for the numerical method. The average percent difference between the solid dock setup numerical and experimental tests for the significant wave height test and the wave period test are displayed in Figure 22.

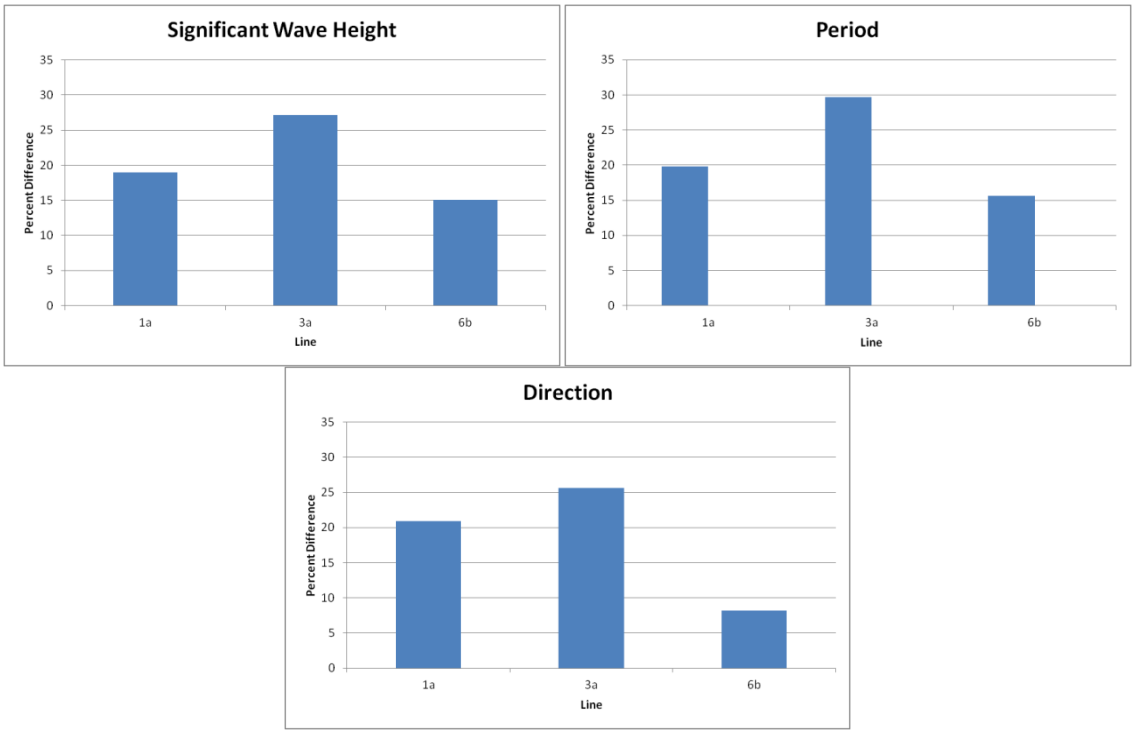

Figure 22. Percent Difference between Numerical and Experimental Tests

Some of the percent difference between the numerical and experimental tests could be due to the fact that the mass properties and distribution in the experimental model and the numerical model were different. The drafts of the model and prototype were modeled but the mass distribution is slightly different. This is believed to be one contributor to the differences between the model and the experiment. Also, the model ship did not have a superstructure. A superstructure would affect the ship's moment of inertia.

The numerical data showed more consistency between the tests at each line, and the numerical data also shows that the average load is lower throughout the tests for each line compared to the experimental data.

5.2 Dock Types

The experimental data also showed that the bow lined received the greatest variation in loads in both the significant wave height test and the wave period test, as shown in Figure 23 and Figure 24. The range of data points in the wave period test on the pile dock showed the greatest standard deviation with 41.6 kips. In both dock setups and in both the significant wave height and wave period tests, the greatest standard deviation occurred in line 1a. These tests show that the bow line is most affected by changes in wave conditions.

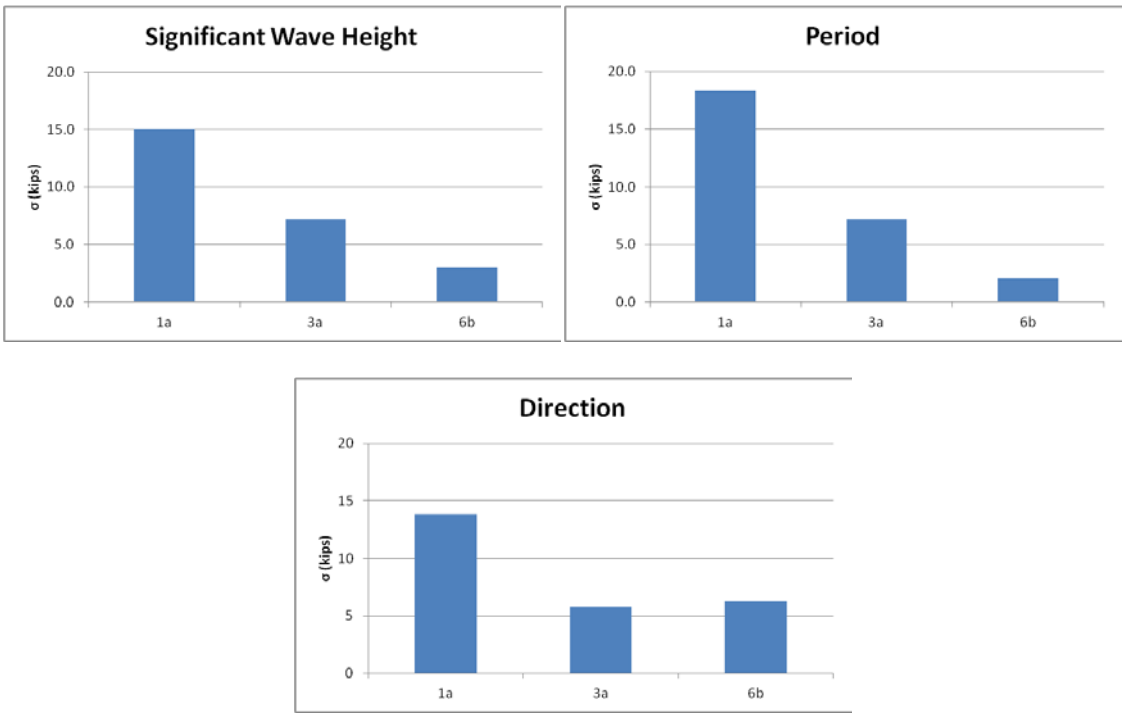

Figure 23. Standard Deviation in Experimental Data of Solid Wall Dock

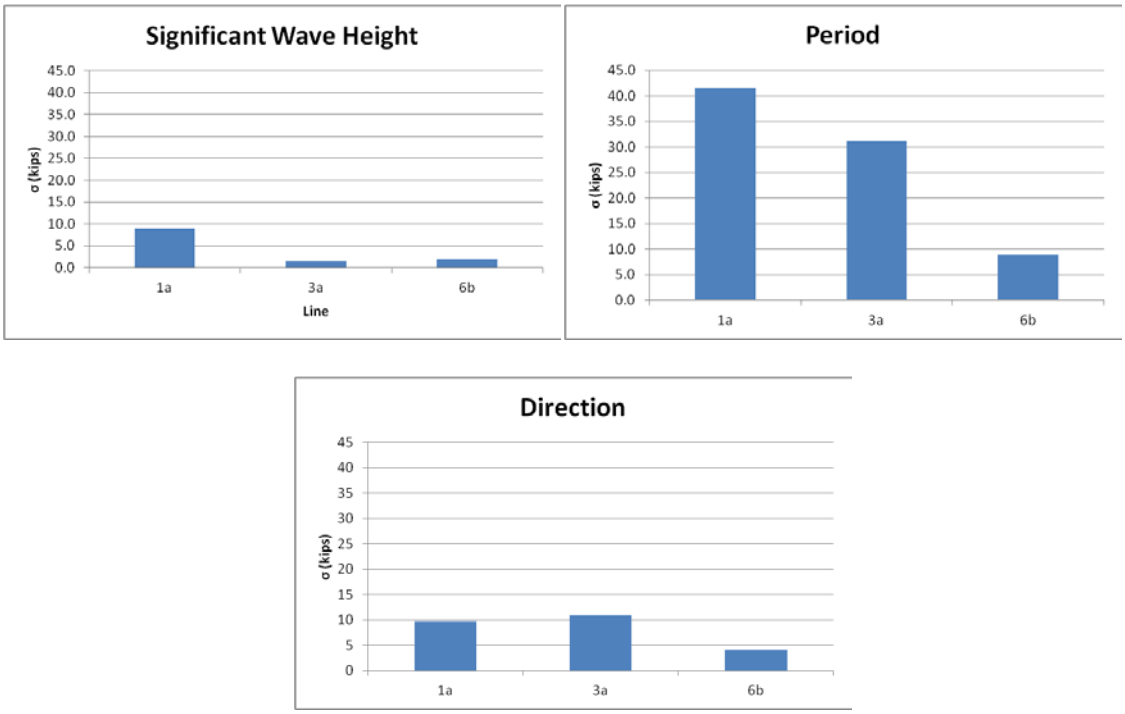

Figure 24. Standard Deviation in Experimental Data of Pile Dock

5.3 Repeatability

The base case with a significant wave height of 6 ft and a wave period of 12 s from tests 3, 21 and 36 from the experimental data is used to determine the repeatability. The results of the tests can be viewed in Figure 25. The average load in lines 1a, 3a, and 6b for Tests 3, 21, and 36 are from the experimental solid dock setup and the experimental pile dock setup test conditions. Test 3 of the solid dock configuration was omitted. From the data available however, the standard deviation for forces on lines 1a, 3a and 6b on the solid dock setup are 2, 2, and 8 kips, respectively. The standard deviations on the same lines on the pile dock setup are 8, 7, and 4 kips respectively. The percent difference between the solid dock setup and the numerical simulation for lines

1a, 3a, and 6b are 36%, 32%, and 11% respectively. The percent difference between the pile dock setup and the solid dock setup on lines 1a, 3a, and 6b are 24%, 12%, and 16%, respectively. A numerical simulation of the pile dock setup was not performed, so there is no comparison between the experimental pile dock setup and the numerical pile dock setup.

The percent difference between the two average loads in the solid dock configuration was 3%, 4% and 22% for lines 1a, 3a, and 6b, respectively. The percent difference between the highest and lowest average load amongst the base cases for each line were 26%, 27%, and 13% for lines 1a, 3a, and 6b, respectively. From these differences, it was concluded that the experiment had reasonable repeatability.

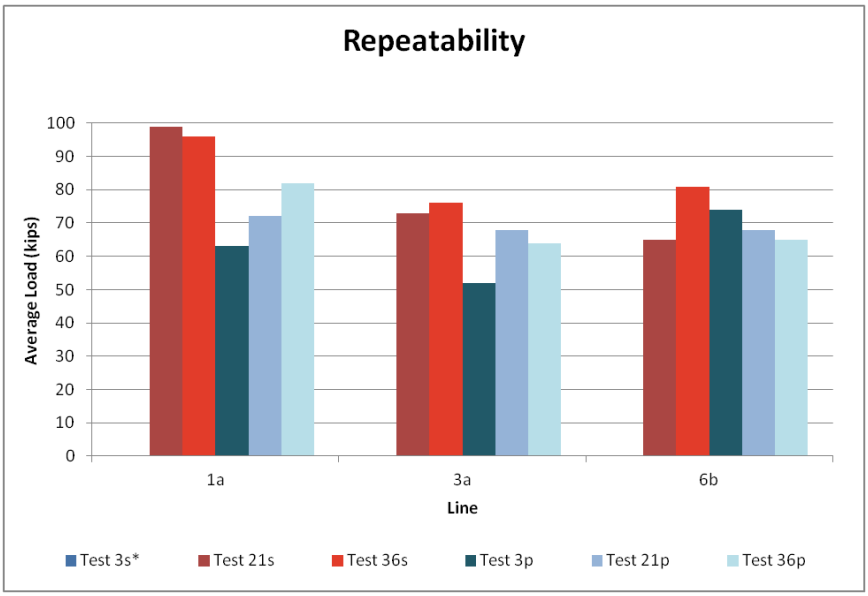

Figure 25. Repeatability of Mooring Line Forces.
Note: "s," and "p" denotes that the test is either for the solid dock setup, pile dock setup, or a numerical model, respectively.
*Test 3s data was omitted.

6. CONCLUSIONS AND RECOMMENDATIONS

6.1 Conclusions

The overall forces on mooring lines moored to a dock increases as the significant wave height and wave period increases. The upward trend in loads as these wave properties intensify is shown in both the bow lines and the spring lines; however, the stern line does not display this trend. Wave direction does not show any obvious trends as the angle changes. The spring lines do not show a consistent increase in load as the wave direction approaches from the bow or stern.

The type of dock, solid and pile, does not change the trends in loads. Both the pile dock and solid dock setups show the same pattern of loads on mooring lines as the significant wave height or wave period increases. However, the pile dock does show a decrease in loads for all lines, especially in the wave period test on the spring line, which had a percent difference between the corresponding line on the solid dock setup of 48%. This was the greatest load difference between the two setups and the wave conditions.

However, the line 1a showed the greatest range in loads in all tests, for both dock setups and wave types. The greatest standard deviation observed in line 1a occurred in the pile dock setup on the wave period test with 41.6 kips. So, the bow line is shown to be most affected by changes in wave types.

The numerical model showed the same trends as the experiments. Simulations showed an increase in loads in all lines as either the significant wave height increased or the wave period increased. However, the overall load for each line throughout all tests

was lower compared to the experimental data. The percent difference between the numerical and experimental results ranged from 36% to 17%. One of the possible factors that led to the disparity was that the mass properties and distribution in the experimental model and the numerical model were different. The numerical program assumed a moment of inertia for the prototype container vessel; however, the model's actual moment of inertia was not determined. The lack of a superstructure on the model vessel would have also affected the results due to the changes it would cause in the moment of inertia.

6.2 Recommendations

Future improvements to the current work can include changes to how the mooring system is modeled. Assumptions such as the exact locations of fenders and mooring line connections were made. The mooring line arrangement for a certain class of ship could more accurately show the effects of different characteristics of waves have on each individual line. Modeling for a specific ship will also provide more accurate data when comparing to a numerical simulation. The physical model and the numerical model ship will have the exact same such as dimensions and mass properties, which could lead to a better comparison between the programmed simulation and the experiment.

Further research can be performed to include different type of mooring lines. In this thesis, one type of mooring line was used throughout the experiment. Different lines of various materials and breaking strengths should be tested. This analysis can show

optimal mooring line characteristics and help determine the most cost efficient arrangement. These results can be compared to those in this thesis.

REFERENCES

Felderhoff, C. (2012). Personal Communication. College Station, TX: Offshore Technology Research Center, Texas A&M University.

Fernandes, A., Vechhio, C., & Gustavo, C. (1998). Mechanical Properties of Polyester Mooring Cables. *International Offshore and Polar Engineering Conference.* Montreal, Canada.

Hanes Supply Inc. (2002). *Wire Rope*. Retrieved from http://www.hanessupply.com/content/catalog pdfs/01-wrope.60 2002 200603.pdf

Hughes, S. A. (1993). *Physical Models and Laboratory Techniques in Coastal Engineering.* Singapore: World Scientific Publishing.

Mansard, E., & Funke, E. (1980). The Measurement of Incident and Reflected Spectra Using a Least Squares Method. *ICCE, Coastal Engineering Chapter.* Sydney: ASCE.

Mansard, E., & Pratte, B. (1982). Moored Ship Response in Irregular Waves. *International Conference on Coastal Engineering.* Cape Town, South Africa: Coastal Engineering Research Council.

Marin. (2012). *ANYwiki.* Retrieved 2013, from http://wiki.marin.nl/index.php/ANYwiki

Pena, E., Ferreras, J., & Sanchez-Tembleque, F. (2011). Experimental study on wave transmission coefficient, mooring lines and module connector forces with different designs of floating breakwaters. *Ocean Engineering , 38* (10), 1150-1160.

Randall, R., Zhi, Y., & Luai, A. (2012). *Model Testing of Motions of Ship Moored at Dock.* Final Report, PND Engineers.

Samson Rope. (2011). *Commercial Marine Product and Technical Guide.* Retrieved 2013, from http://www.samsonropecatalogs.com/index.cfm/catalog/Commercial_Marine_2012

Szelangiewicz, T. (1996). Loads in Mooring Lines of Mooring Positioning System of a Vessel. *International Offshore and Polar Engineering Conference.* Los Angeles, USA.

van der Molen, W., Rossouw, M., Phelp, D., Tulsi, K., & Terblanche, L. (2010). Innovative Technologies to Accurately Model Waves and Moored Ship Motions. *Science Real and Relevant Conference.* Pretoria, South Africa: CSIR.

APPENDIX A

Mooring line and fender force comparison plots between solid and pile dock configurations are shown in Appendix Figures A-1 through A-18. Only results of the tests analyzed in this thesis are shown. The test number is labeled as the heading and is the same as those reported in (Randall, Zhi, & Luai, 2012). Tests 1 to 4 on the solid dock configuration were omitted due to load cell malfunction, and tests 5 to 23 fender data on the solid dock configuration were also omitted due to load cells not working properly. The data shows the prototype loads on the mooring line and fenders as a function of time. At the bottom of the figures are the maximum and average loads for each line for each dock configuration.

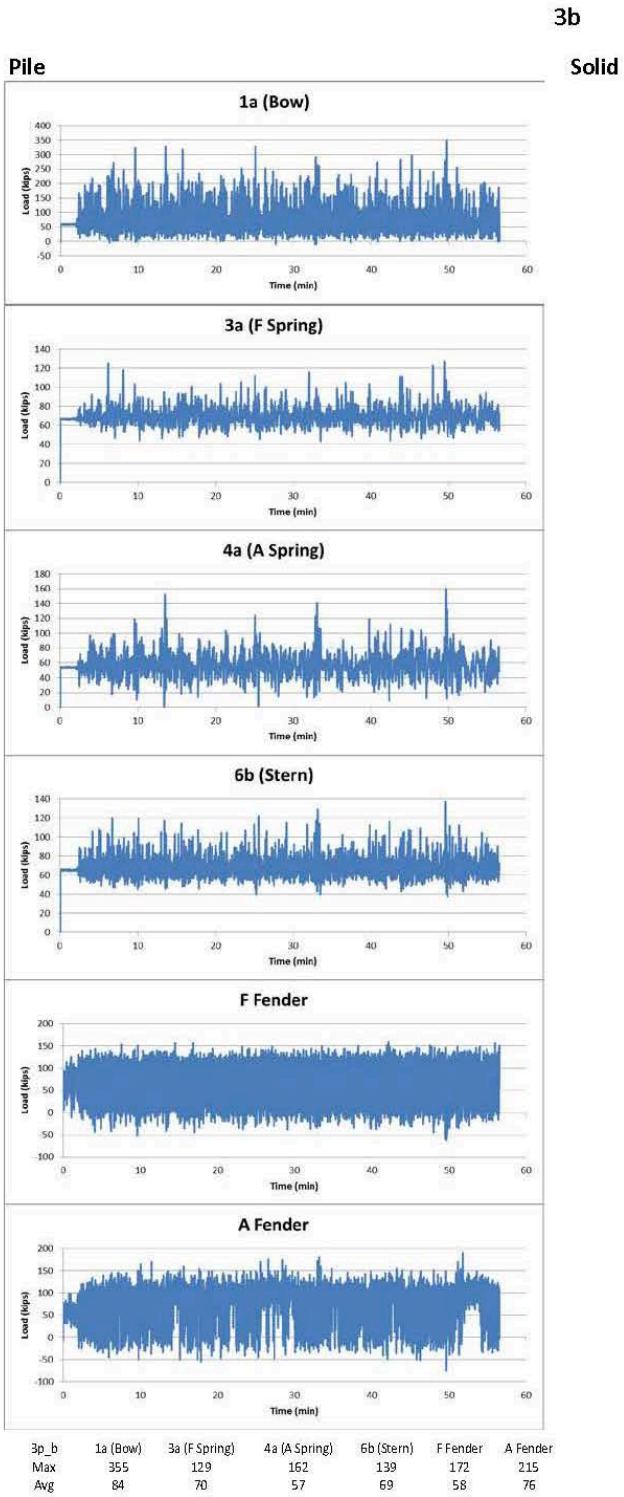

3p_b	1a (Bow)	3a (F Spring)	4a (A Spring)	6b (Stern)	F Fender	A Fender
Max	355	129	162	139	172	215
Avg	84	70	57	69	58	76

Figure A-1. Test 3. Significant wave height: 6 ft, Peak wave period: 12 sec, Wave Direction: 0°. Note: solid dock data unavailable.

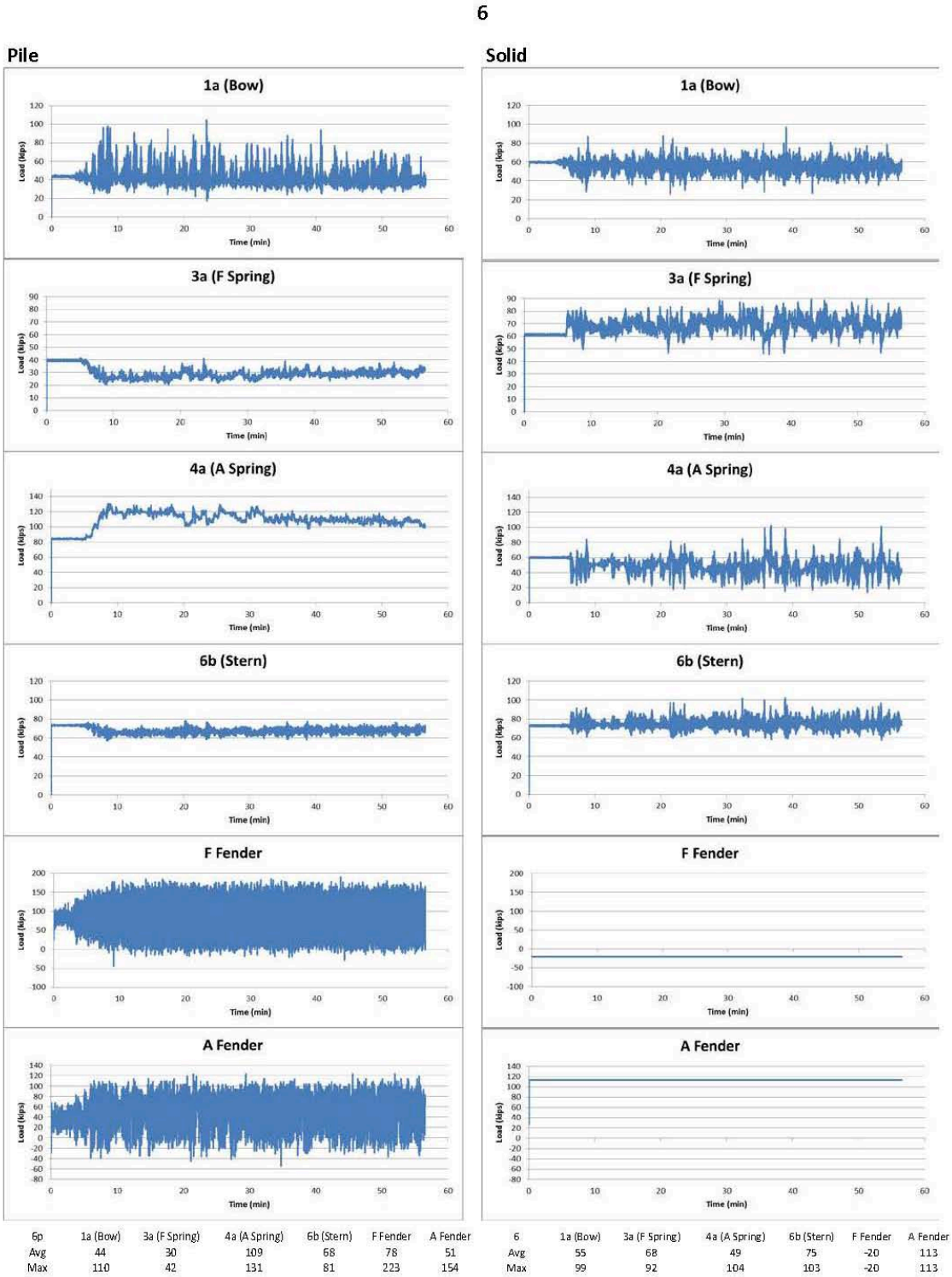

6p	1a (Bow)	3a (F Spring)	4a (A Spring)	6b (Stern)	F Fender	A Fender
Avg	44	30	109	68	78	51
Max	110	42	131	81	223	154

6	1a (Bow)	3a (F Spring)	4a (A Spring)	6b (Stern)	F Fender	A Fender
Avg	55	68	49	75	-20	113
Max	99	92	104	103	-20	113

Figure A-2. Test 6. Significant wave height: 6 ft, Peak wave period: 4 sec, Wave Direction: 0°. Note: fender data for solid dock data unavailable.

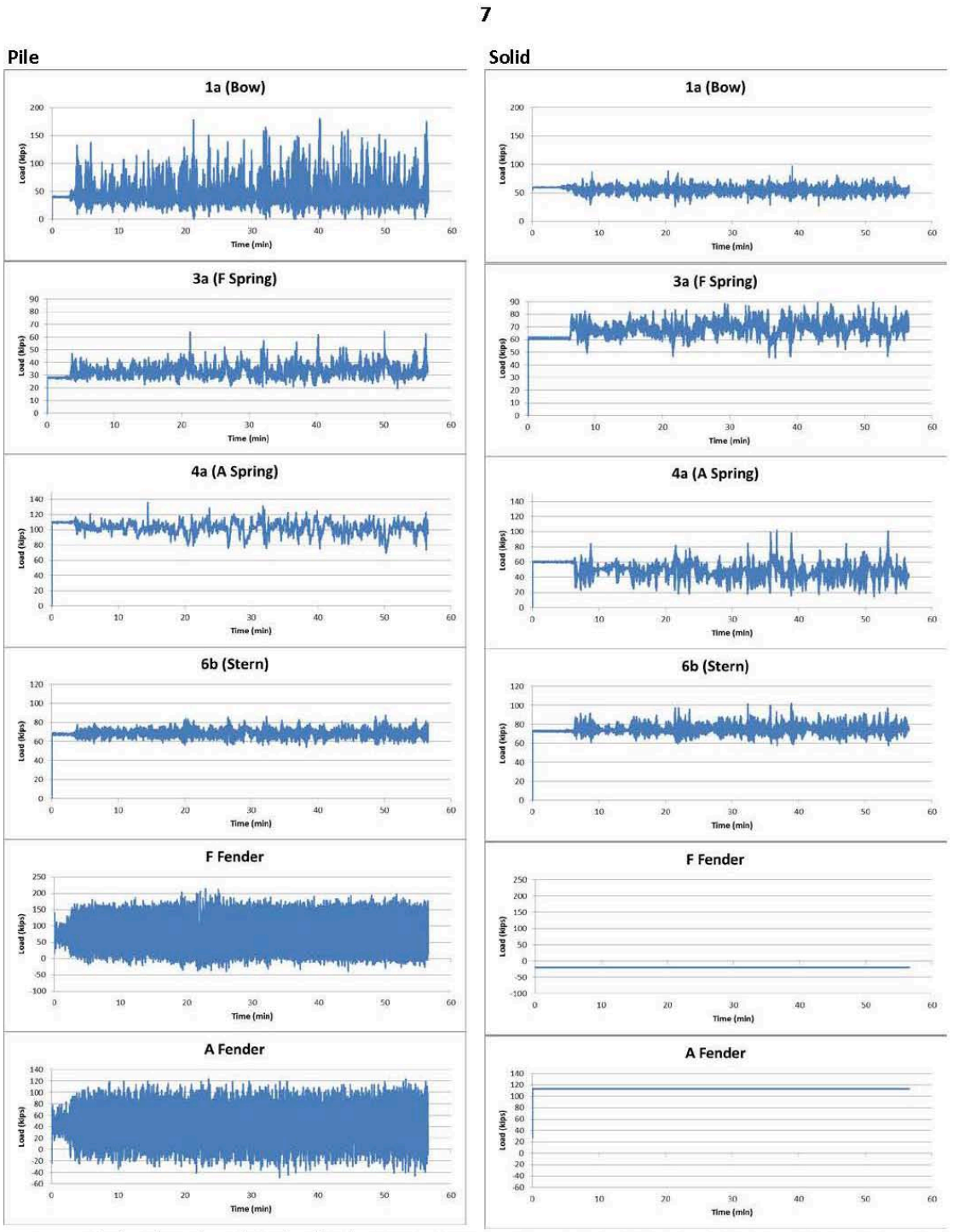

7p	1a (Bow)	3a (F Spring)	4a (A Spring)	6b (Stern)	F Fender	A Fender
Avg	51	33	103	69	68	47
Max	184	65	137	91	237	154

7	1a (Bow)	3a (F Spring)	4a (A Spring)	6b (Stern)	F Fender	A Fender
Avg	55	68	49	75	-20	113
Max	99	92	104	103	-20	113

Figure A-3. Test 7. Significant wave height: 6 ft, Peak wave period: 6 sec, Wave Direction: 0°. Note: fender data for solid dock data unavailable.

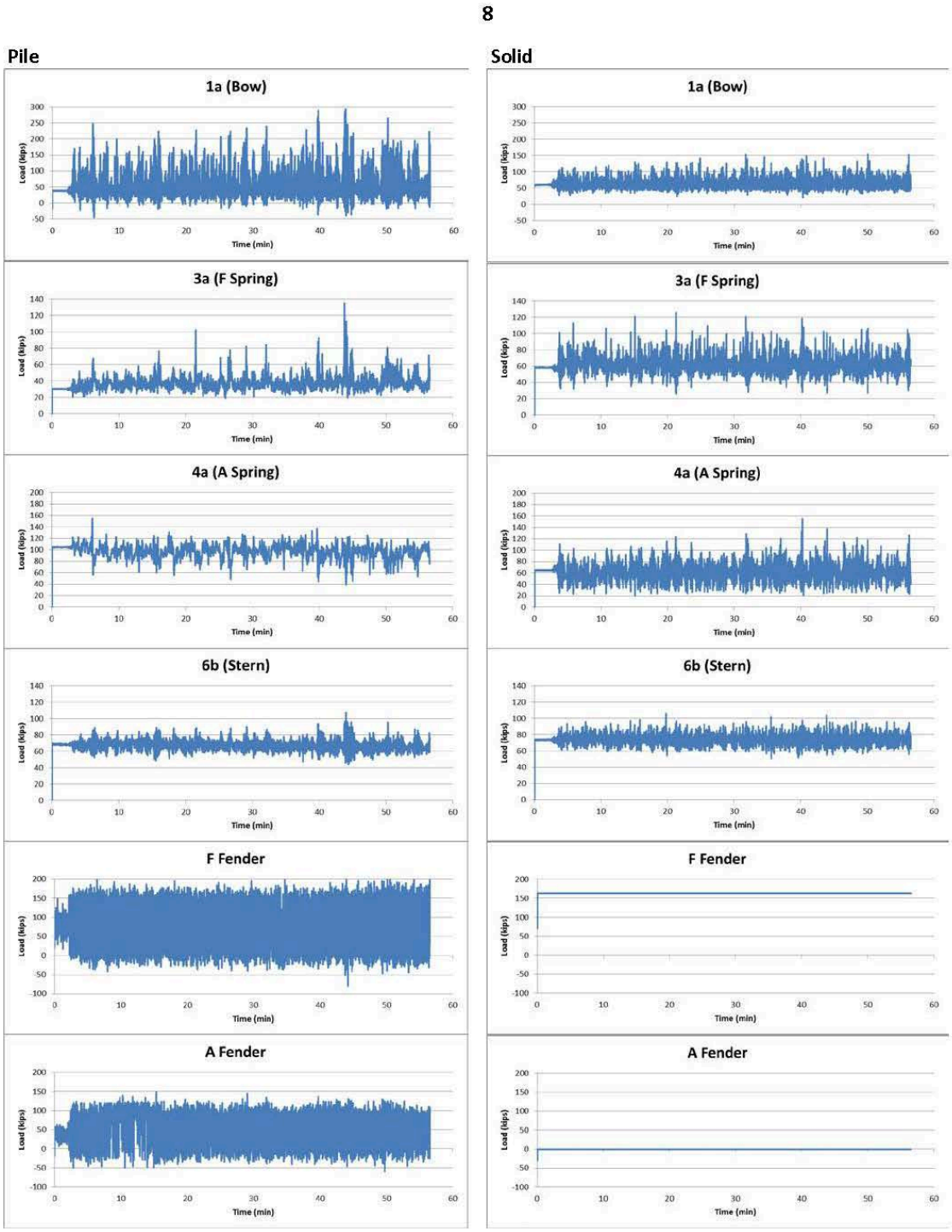

8p	1a (Bow)	3a (F Spring)	4a (A Spring)	6b (Stern)	F Fender	A Fender
Avg	64	38	97	68	61	55
Max	292	136	155	109	335	195

8	1a (Bow)	3a (F Spring)	4a (A Spring)	6b (Stern)	F Fender	A Fender
Avg	66	62	62	74	163	0
Max	161	129	159	106	163	0

Figure A-4. Test 8. Significant wave height: 6 ft, Peak wave period: 8 sec, Wave Direction: 0°. Note: fender data for solid dock data unavailable.

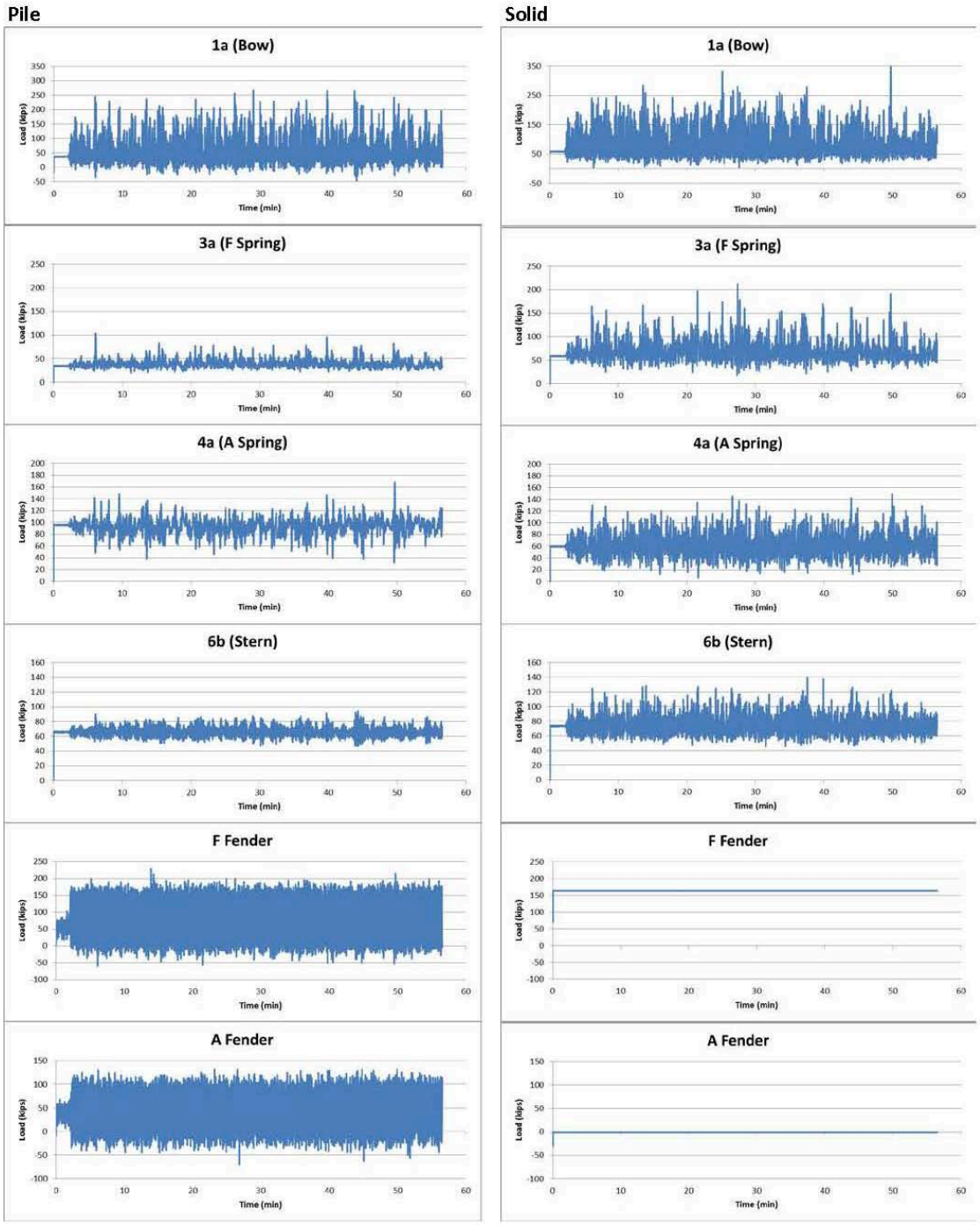

9p	1a (Bow)	3a (F Spring)	4a (A Spring)	6b (Stern)	F Fender	A Fender
Avg	63	40	93	66	56	46
Max	275	104	169	102	268	164

9	1a (Bow)	3a (F Spring)	4a (A Spring)	6b (Stern)	F Fender	A Fender
Avg	87	70	62	76	163	0
Max	351	213	149	140	163	0

Figure A-5. Test 9. Significant wave height: 6 ft, Peak wave period: 10 sec, Wave Direction: 0°. Note: fender data for solid dock data unavailable.

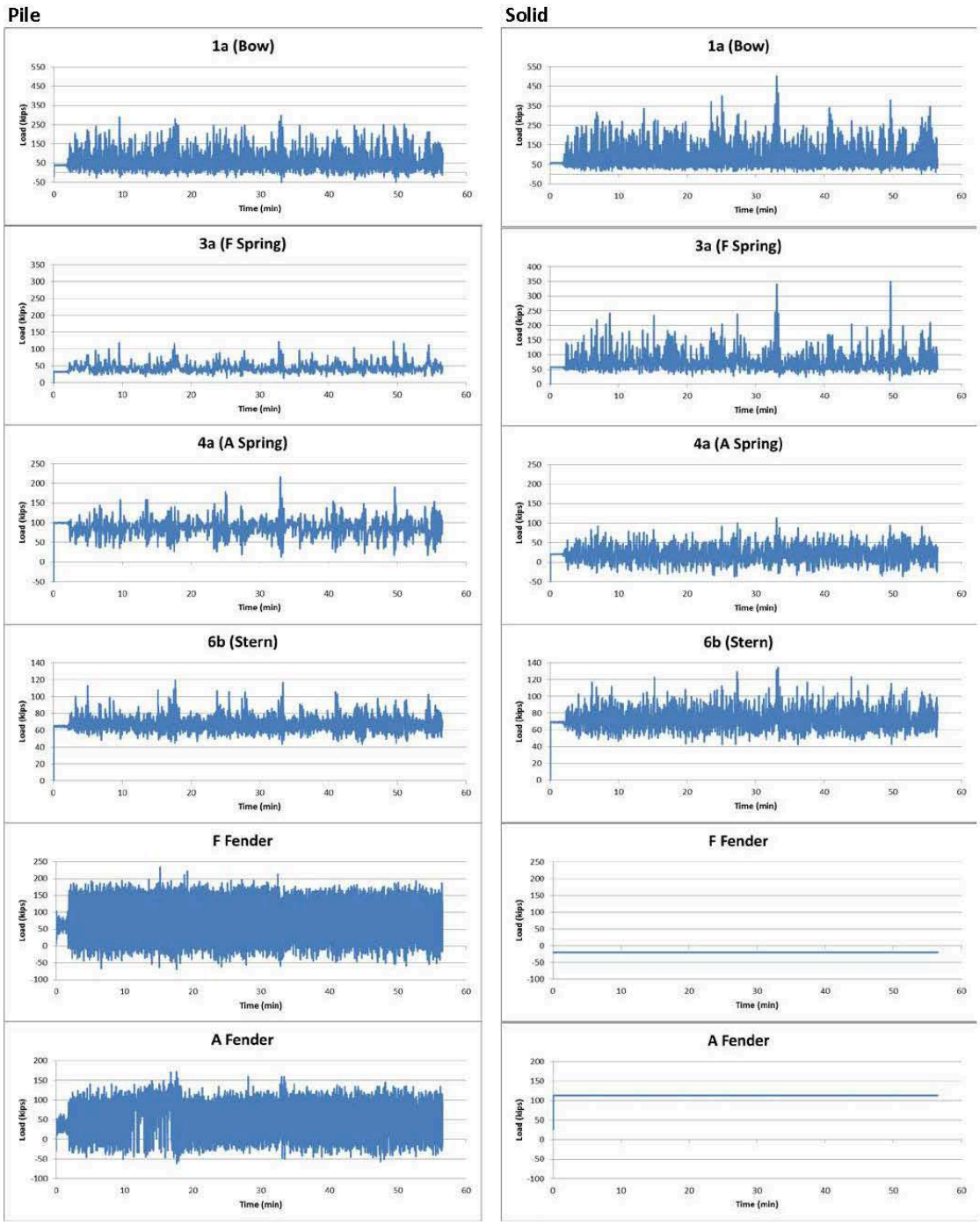

10p	1a (Bow)	3a (F Spring)	4a (A Spring)	6b (Stern)	F Fender	A Fender
Avg	68	45	88	68	59	58
Max	312	123	219	120	291	225

10	1a (Bow)	3a (F Spring)	4a (A Spring)	6b (Stern)	F Fender	A Fender
Avg	97	77	19	72	-20	113
Max	510	352	114	137	-20	113

Figure A-6. Test 10. Significant wave height: 6 ft, Peak wave period: 14 sec, Wave Direction: 0°. Note: fender data for solid dock data unavailable.

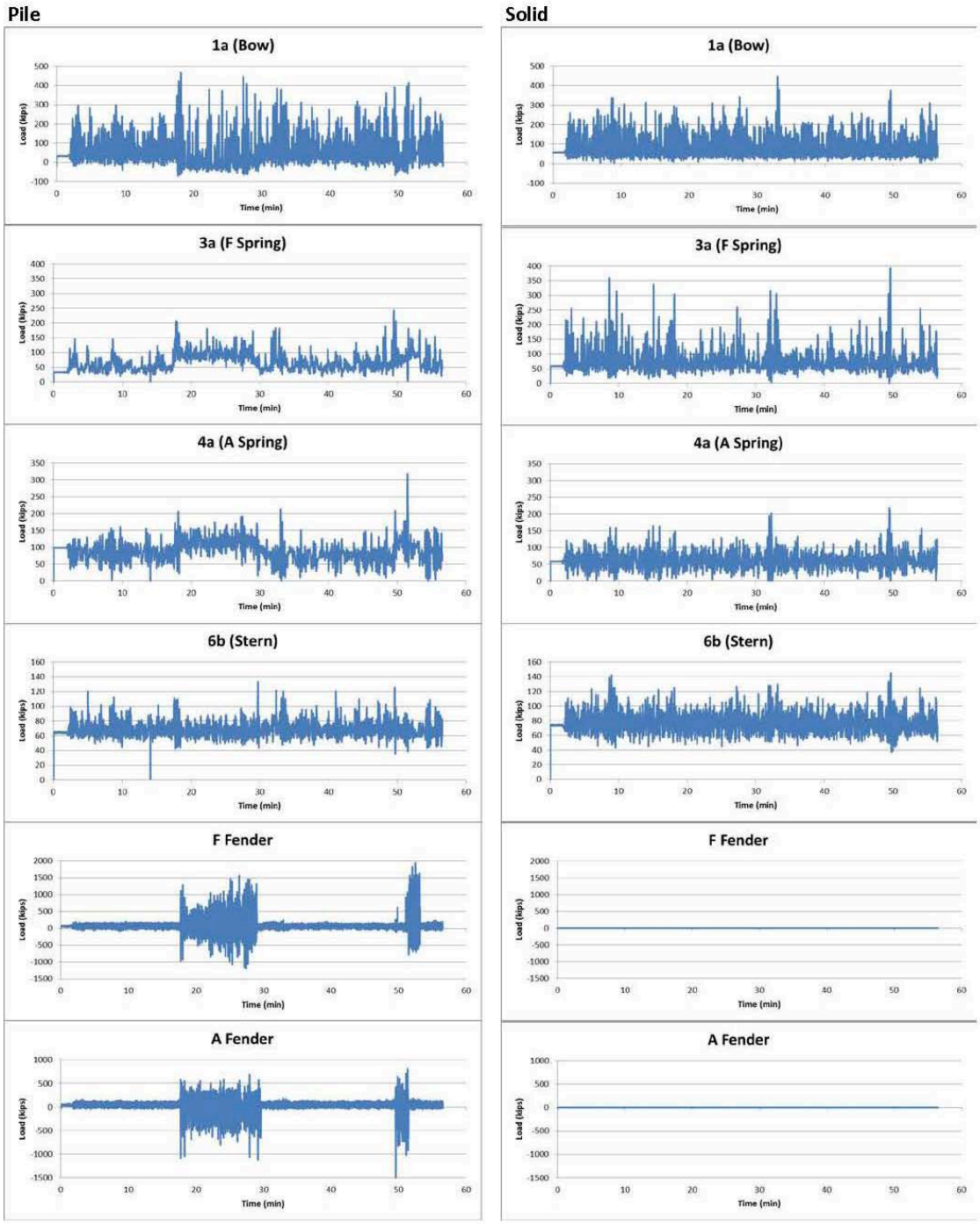

11p	1a (Bow)	3a (F Spring)	4a (A Spring)	6b (Stern)	F Fender	A Fender
Avg	74	68	89	69	65	28
Max	470	244	320	134	1975	1152

11	1a (Bow)	3a (F Spring)	4a (A Spring)	6b (Stern)	F Fender	A Fender
Avg	96	79	61	78	3	0
Max	450	396	219	150	3	0

Figure A-7. Test 11. Significant wave height: 6 ft, Peak wave period: 16 sec, Wave Direction: 0°. Note: fender data for solid dock data unavailable.

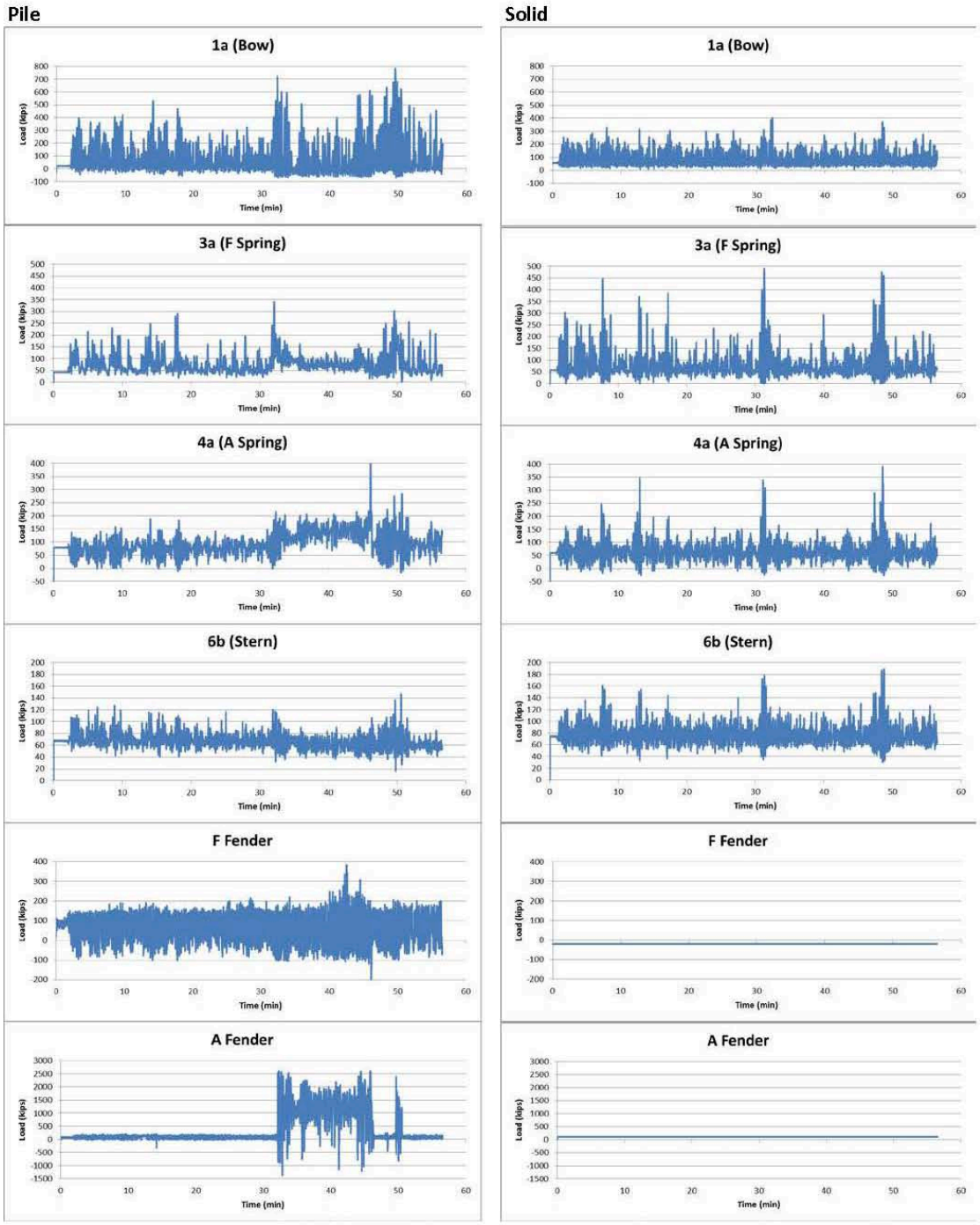

12p	1a (Bow)	3a (F Spring)	4a (A Spring)	6b (Stern)	F Fender	A Fender
Avg	95	78	94	67	46	396
Max	803	342	403	152	407	3096

12	1a (Bow)	3a (F Spring)	4a (A Spring)	6b (Stern)	F Fender	A Fender
Avg	94	80	64	78	-20	113
Max	405	492	394	188	-20	113

Figure A-8. Test 12. Significant wave height: 6 ft, Peak wave period: 18 sec, Wave Direction: 0°. Note: fender data for solid dock data unavailable.

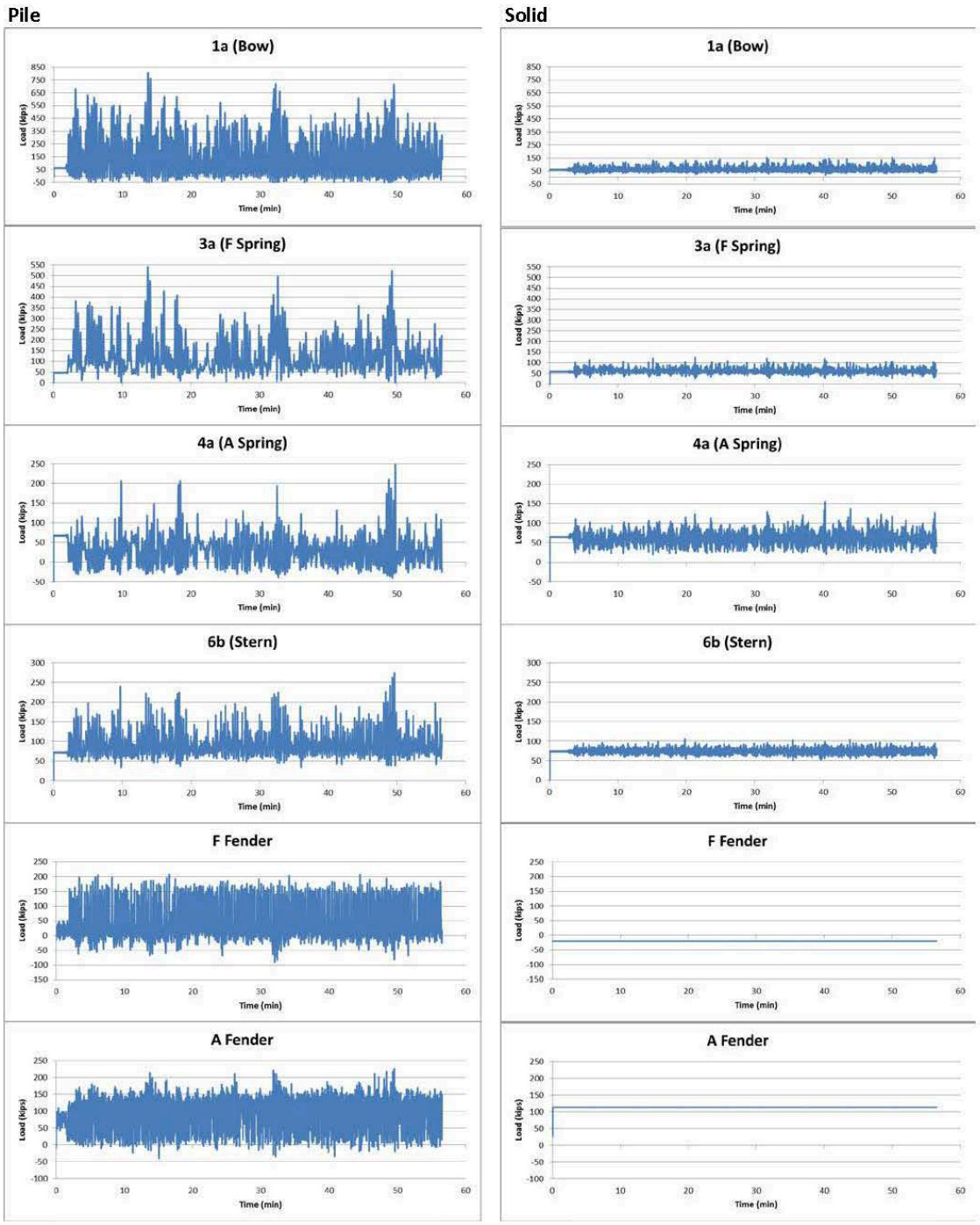

13p	1a (Bow)	3a (F Spring)	4a (A Spring)	6b (Stern)	F Fender	A Fender
Avg	175	121	29	93	37	97
Max	819	543	251	282	264	276

13	1a (Bow)	3a (F Spring)	4a (A Spring)	6b (Stern)	F Fender	A Fender
Avg	66	62	62	74	-20	113
Max	161	129	159	106	-20	113

Figure A-9. Test 13. Significant wave height: 6 ft, Peak wave period: 20 sec, Wave Direction: 0°. Note: fender data for solid dock data unavailable.

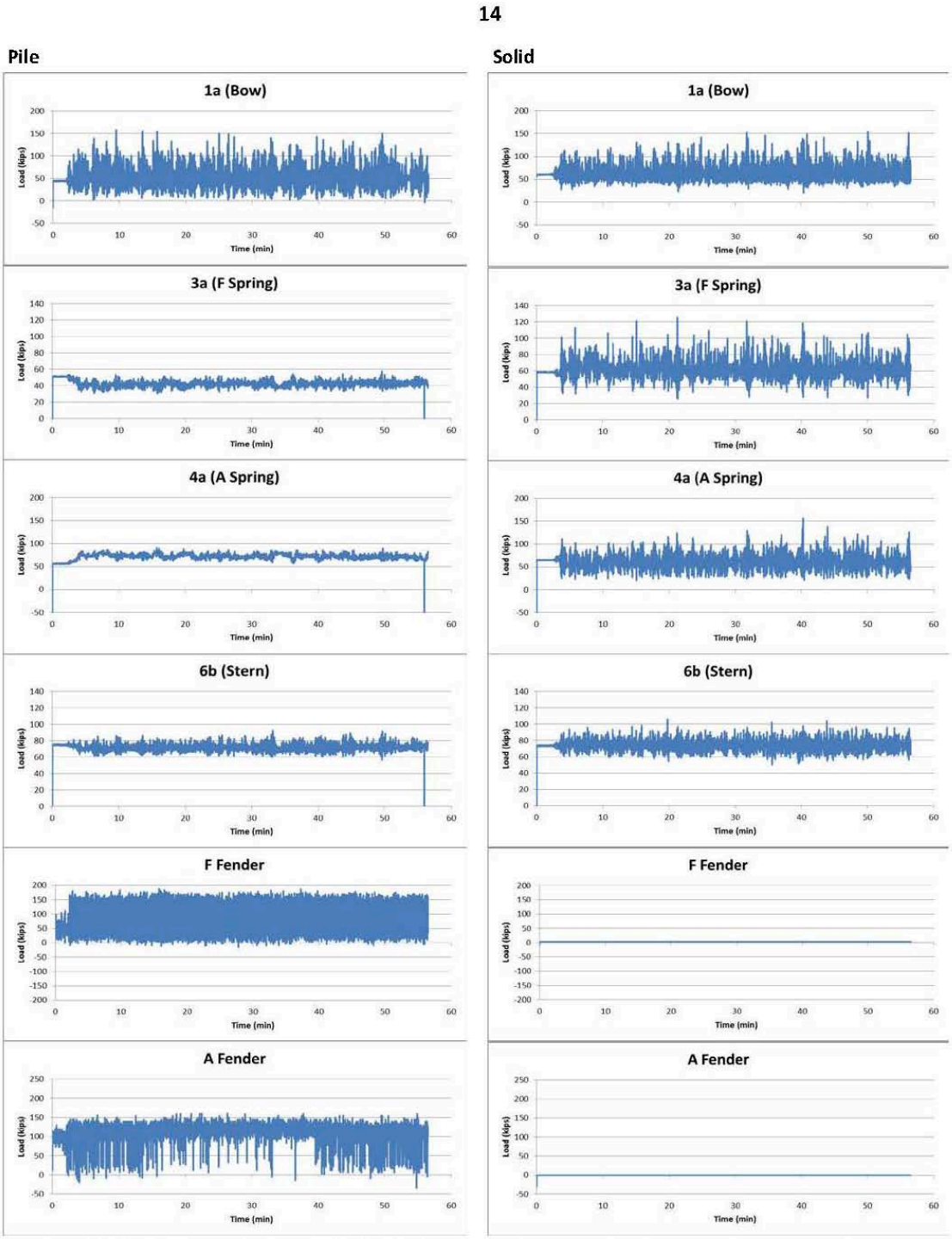

14p	1a (Bow)	3a (F Spring)	4a (A Spring)	6b (Stern)	F Fender	A Fender
Avg	54	43	72	72	80	109
Max	159	58	92	93	205	195

14	1a (Bow)	3a (F Spring)	4a (A Spring)	6b (Stern)	F Fender	A Fender
Avg	66	62	62	74	3	0
Max	161	129	159	106	3	0

Figure A-10. Test 14. Significant wave height: 2 ft, Peak wave period: 12 sec, Wave Direction: 0°. Note: fender data for solid dock data unavailable.

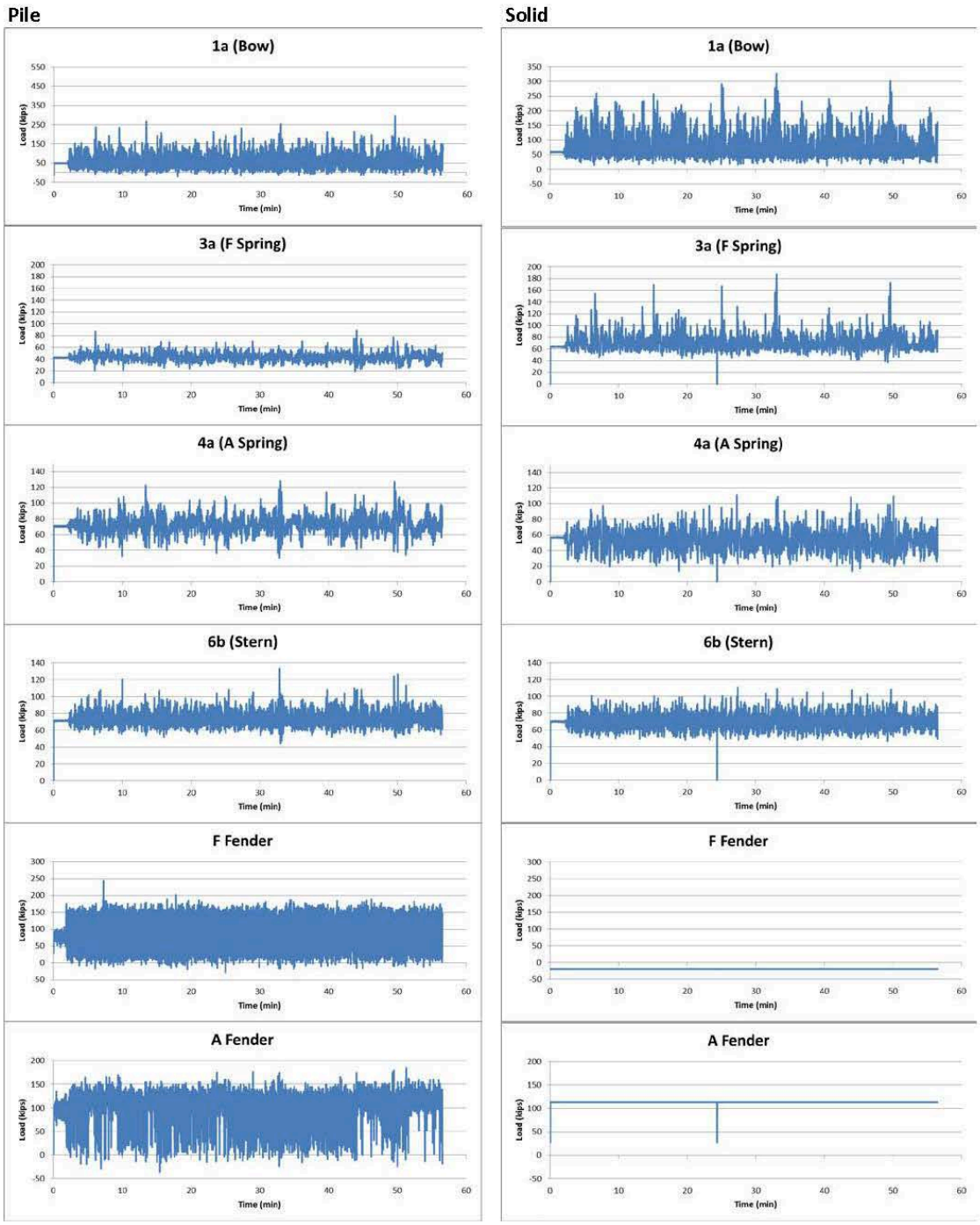

15p	1a (Bow)	3a (F Spring)	4a (A Spring)	6b (Stern)	F Fender	A Fender
Avg	63	44	73	74	75	101
Max	299	89	129	134	297	225

15	1a (Bow)	3a (F Spring)	4a (A Spring)	6b (Stern)	F Fender	A Fender
Avg	83	72	52	71	-20	113
Max	329	188	112	110	-20	113

Figure A-11. Test 15. Significant wave height: 4 ft, Peak wave period: 12 sec, Wave Direction: 0°. Note: fender data for solid dock data unavailable.

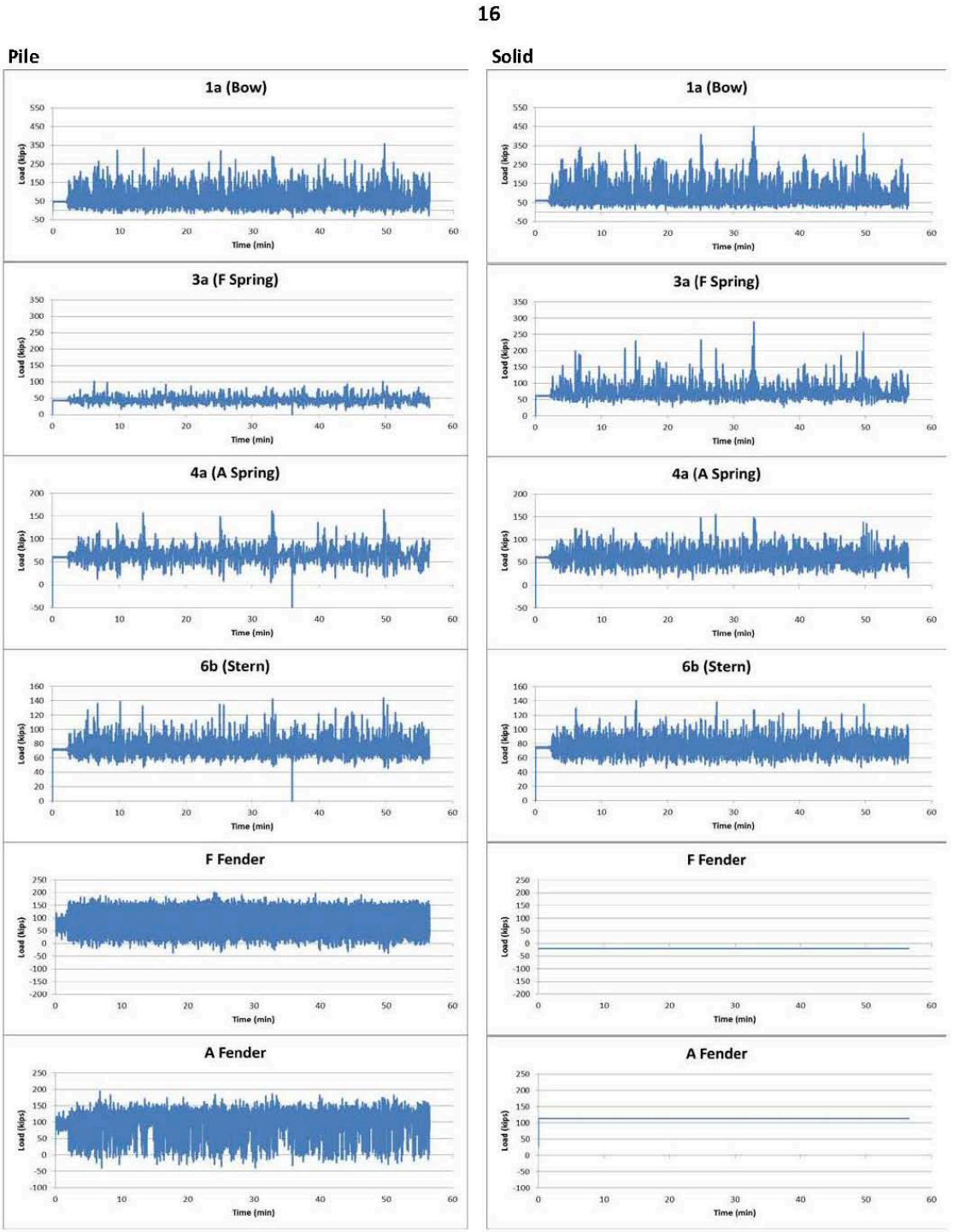

16p	1a (Bow)	3a (F Spring)	4a (A Spring)	6b (Stern)	F Fender	A Fender
Avg	72	46	66	76	74	99
Max	362	102	164	145	311	236

16	1a (Bow)	3a (F Spring)	4a (A Spring)	6b (Stern)	F Fender	A Fender
Avg	96	76	62	77	-20	113
Max	457	290	158	141	-20	113

Figure A-12. Test 16. Significant wave height: 8 ft, Peak wave period: 12 sec, Wave Direction: 0°. Note: fender data for solid dock data unavailable.

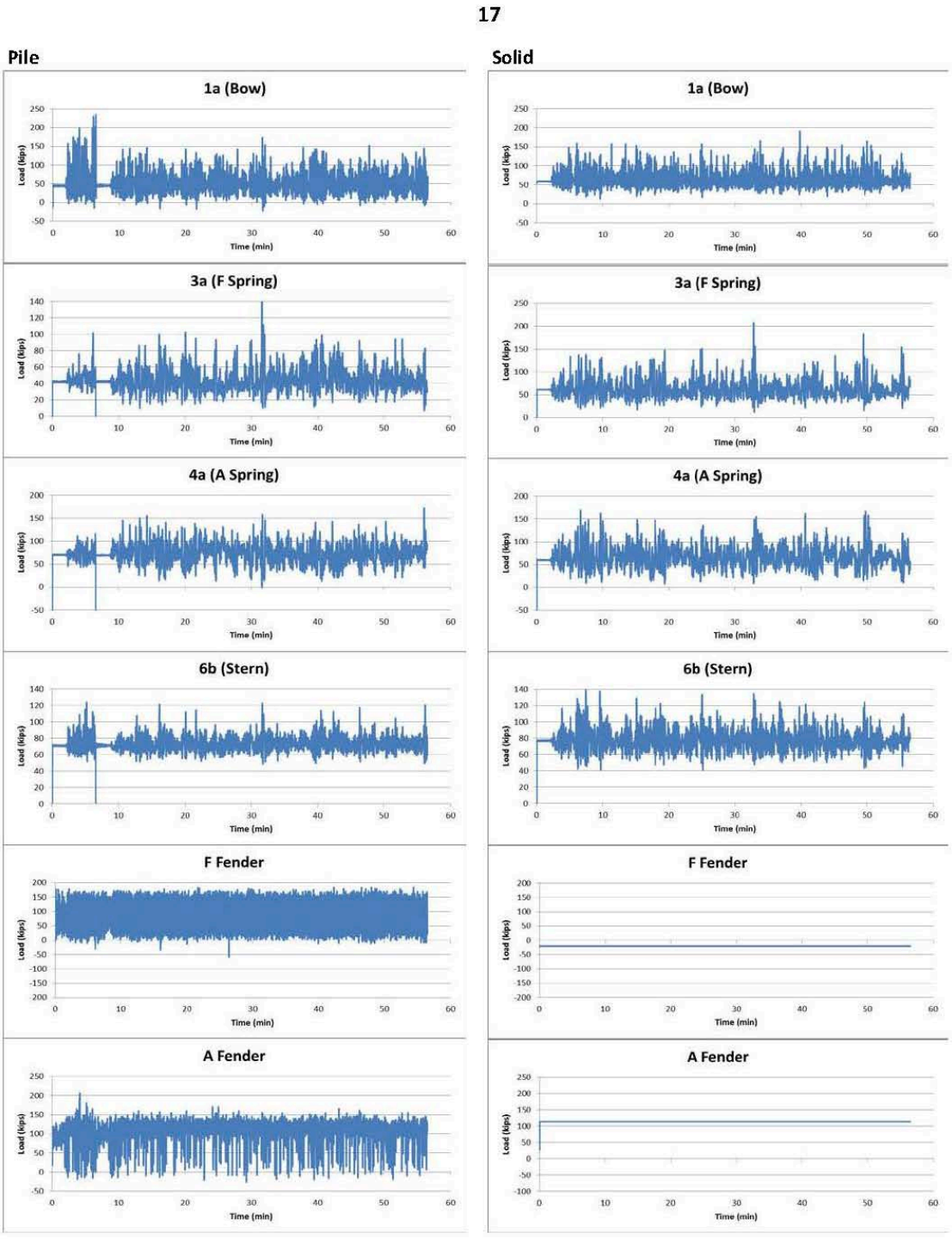

17p	1a (Bow)	3a (F Spring)	4a (A Spring)	6b (Stern)	F Fender	A Fender
Avg	54	45	72	73	79	107
Max	236	141	172	125	208	276

17	1a (Bow)	3a (F Spring)	4a (A Spring)	6b (Stern)	F Fender	A Fender
Avg	67	64	66	78	-20	113
Max	192	208	173	145	-20	113

Figure A-13. Test 17. Significant wave height: 6 ft, Peak wave period: 12 sec, Wave Direction: +30°. Note: fender data for solid dock data unavailable.

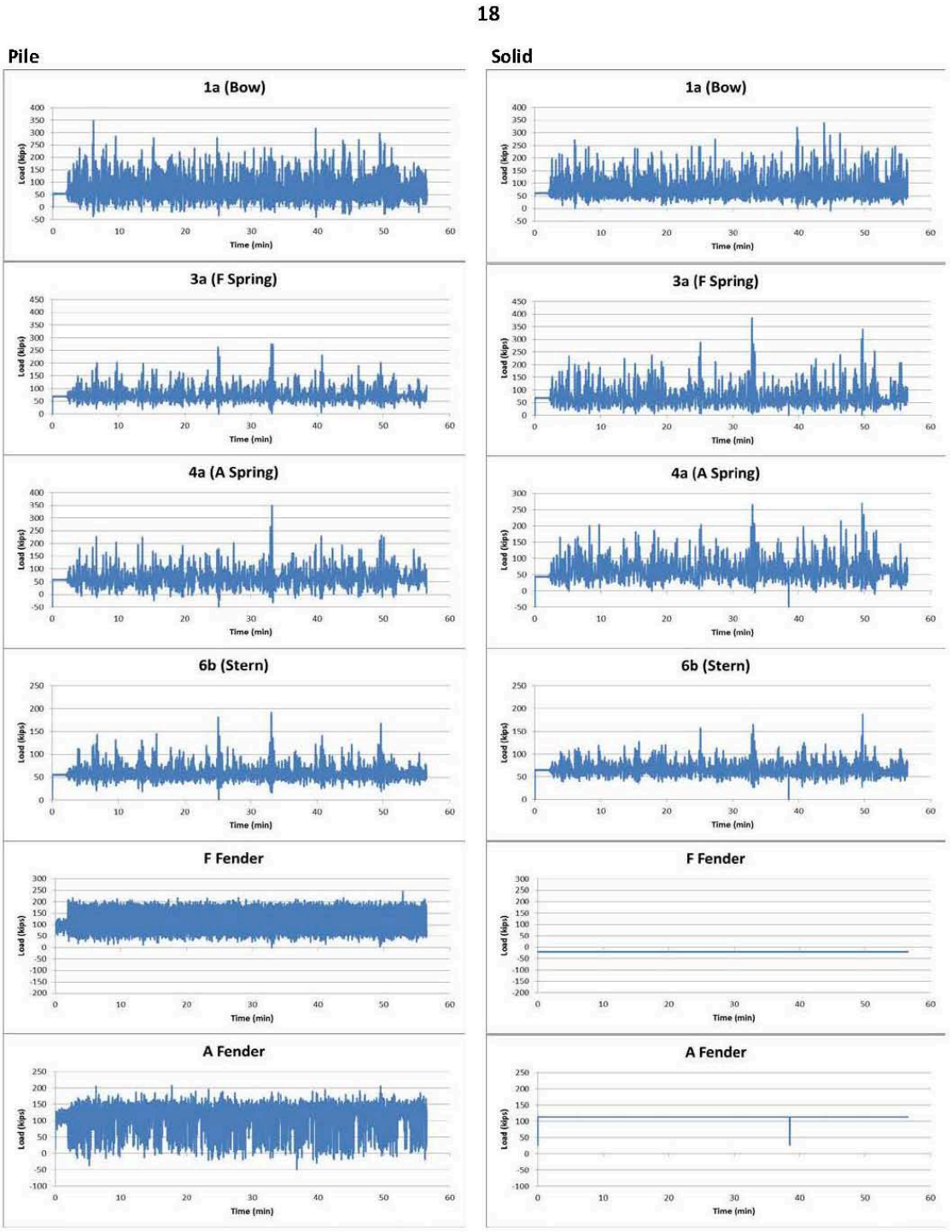

18p	1a (Bow)	3a (F Spring)	4a (A Spring)	6b (Stern)	F Fender	A Fender
Avg	78	77	64	61	112	115
Max	352	280	355	193	330	246

18	1a (Bow)	3a (F Spring)	4a (A Spring)	6b (Stern)	F Fender	A Fender
Avg	85	74	63	68	-20	113
Max	341	389	271	190	-22	113

Figure A-14. Test 18. Significant wave height: 6 ft, Peak wave period: 12 sec, Wave Direction: +15°. Note: fender data for solid dock data unavailable.

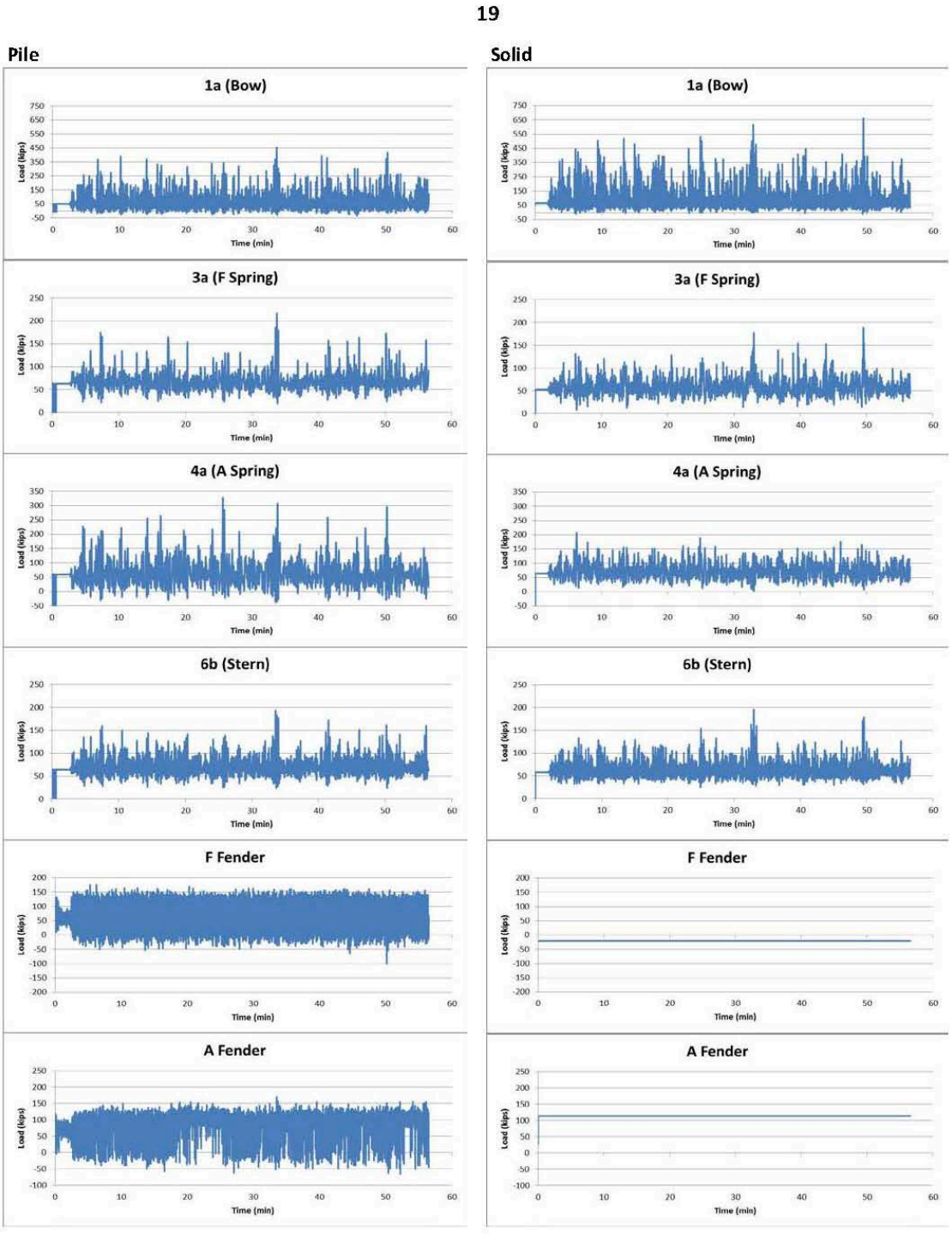

19p	1a (Bow)	3a (F Spring)	4a (A Spring)	6b (Stern)	F Fender	A Fender
Avg	73	69	64	70	57	84
Max	458	218	328	194	197	195

19	1a (Bow)	3a (F Spring)	4a (A Spring)	6b (Stern)	F Fender	A Fende
Avg	102	59	72	64	-20	113
Max	669	189	210	198	-20	113

Figure A-15. Test 19. Significant wave height: 6 ft, Peak wave period: 12 sec, Wave Direction: -15°. Note: fender data for solid dock data unavailable.

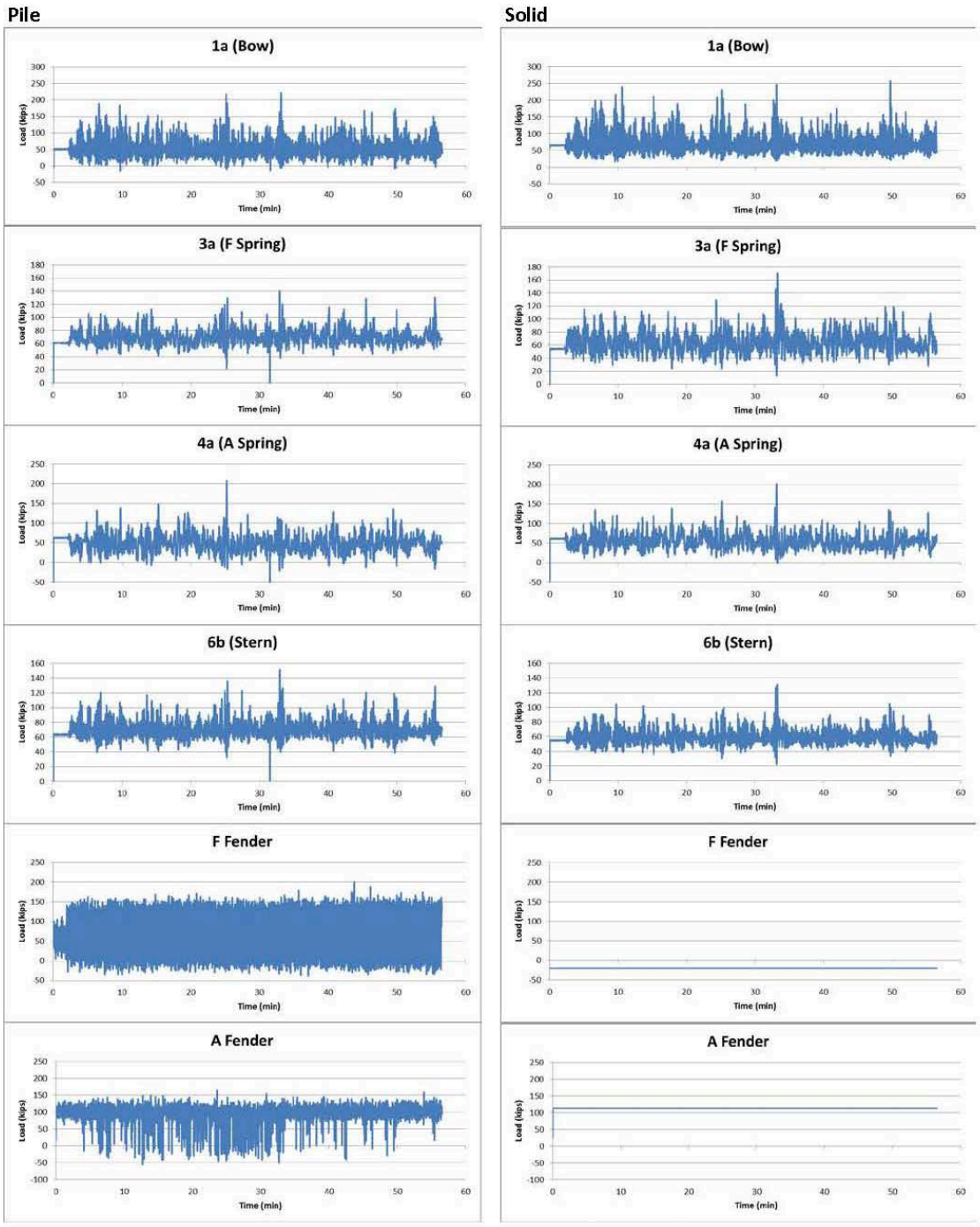

20p	1a (Bow)	3a (F Spring)	4a (A Spring)	6b (Stern)	F Fender	A Fender
Avg	56	70	49	70	62	96
Max	222	141	208	152	221	205

20	1a (Bow)	3a (F Spring)	4a (A Spring)	6b (Stern)	F Fender	A Fender
Avg	73	64	56	59	-20	113
Max	257	171	202	131	-20	113

Figure A-16. Test 20. Significant wave height: 6 ft, Peak wave period: 12 sec, Wave Direction: -30°. Note: fender data for solid dock data unavailable.

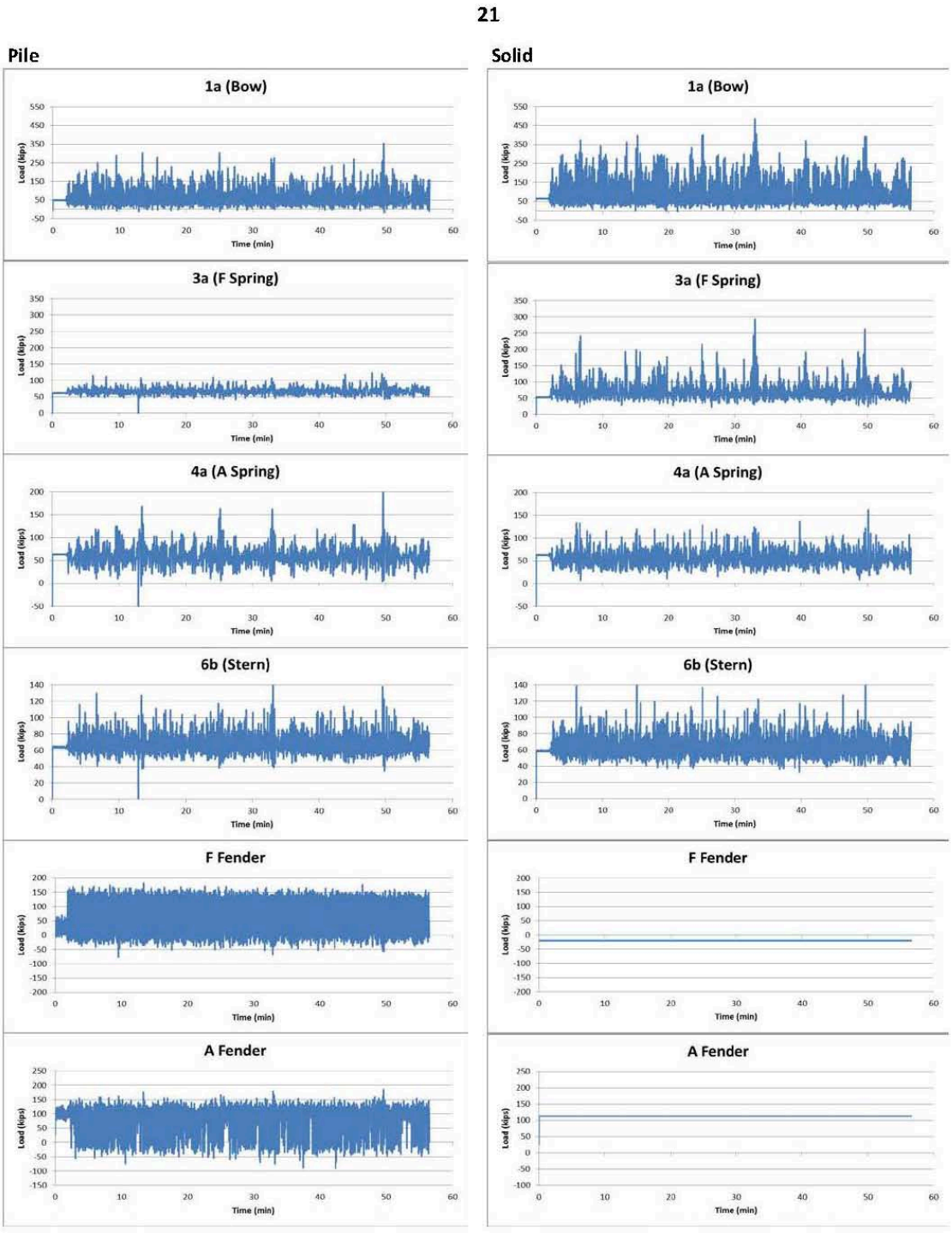

21p	1a (Bow)	3a (F Spring)	4a (A Spring)	6b (Stern)	F Fender	A Fender
Avg	72	68	60	68	58	84
Max	362	123	199	142	243	205

21	1a (Bow)	3a (F Spring)	4a (A Spring)	6b (Stern)	F Fender	A Fende
Avg	99	73	56	65	-20	113
Max	491	296	167	146	-20	113

Figure A-17. Test 21. Significant wave height: 6 ft, Peak wave period: 12 sec, Wave Direction: 0°. Note: fender data for solid dock data unavailable.

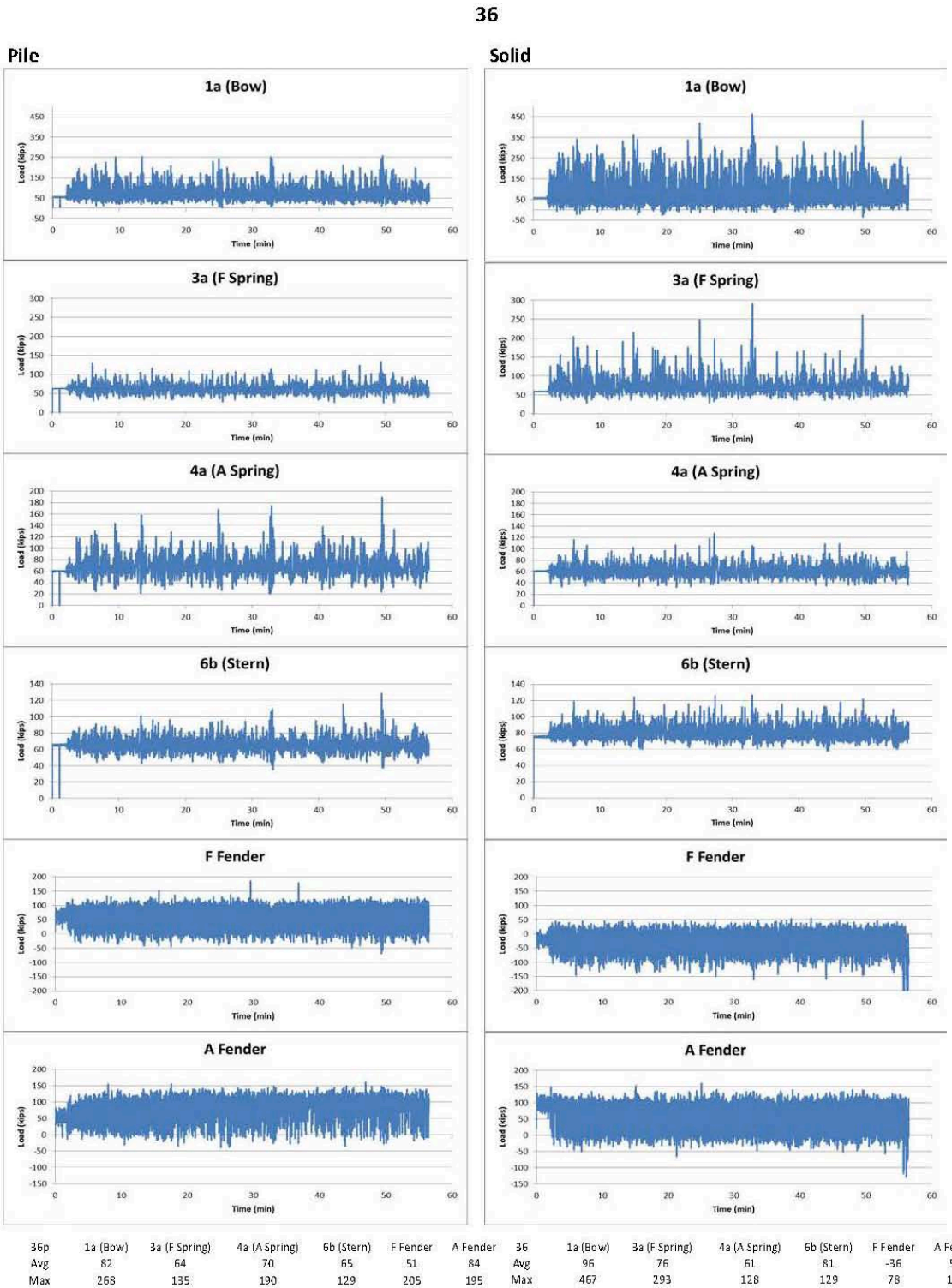

36p	1a (Bow)	3a (F Spring)	4a (A Spring)	6b (Stern)	F Fender	A Fender	36	1a (Bow)	3a (F Spring)	4a (A Spring)	6b (Stern)	F Fender	A Fender
Avg	82	64	70	65	51	84	Avg	96	76	61	81	-36	59
Max	268	135	190	129	205	195	Max	467	293	128	129	78	174

Figure A-18. Test 36. Significant wave height: 6 ft, Peak wave period: 12 sec, Wave Direction: 0°.